# Heterogeneous vanadium catalyzed oxidative cleavage of olefins for sustainable synthesis of carboxylic acids

Rahul Upadhyay,[ab] Rohit Rana,[ab] Aakriti Sood,[a] Vikash Singh,[c] Rahul Kumar,[ab] Vimal Chandra Srivastava[c] and Sushil K. Maurya*[ab]

AUTHOR ADDRESS

[a]Chemical Technology Division, CSIR-Institute of Himalayan Bioresource Technology Palampur, Himachal Pradesh, 176 061, India; [b]Academy of Scientific and Innovative Research (AcSIR), Ghaziabad 201 002, India; [c]Department of Chemical Engineering, Indian Institute of Technology Roorkee, Roorkee, Uttarakhand, 247 667, India.

sushilncl@gmail.com, skmaurya@ihbt.res.in.

## Contents

**1. General Information……...S2**

**2. Catalyst preparation and characterization…….……...……S2-S8**

**3. General synthetic procedure……...S8-S9**

**4. General procedure for catalyst recyclability……...…….....S9**

**5. Optimization table……..S9-S10**

**6. $^{1}$H and $^{13}$C data and spectra…….....S10-S27**

**7. Controlled experiment ESI-MS ……S28**

**8. GC-MS of crude reaction mixture ……S28**

**9. References……S29**

## General Information

High purity solvents were used for all reactions. Silica gel (60-120, 230-400 mesh, S. D. Fine make and spectrochem make) was used for column chromatography. All reactions were monitored by thin-layer chromatography (TLC) using pre-coated silica plates (Merck $F_{254}$, 0.25 mm thickness). NMR solvents were purchased from Sigma Aldrich. $^{1}H$ NMR and $^{13}C$ NMR experiments were performed on Bruker Avance- 600 spectrometers. Mass spectra were recorded on a Q-TOF mass spectrometer.

### Catalyst preparation (Sol-Gel Method)

**Preparation of titanium peroxo-complex solution (A):** To a beaker charged with $Ti(OBu)_4$ was added deionized water and the resulting solution was stirred at 25 $^{o}C$ for 30 min. To this solution was slowly added $H_2O_2$ (30% aq.) that resulted in an orange-coloured titanium peroxo-complex solution.

**Preparation of peroxovanadic solution (B):** $V_2O_5$ was hydrolyzed with deionized water under continuous stirring in a beaker. To this hydrolyzed solution was added $H_2O_2$ (30% aq.) dropwise to furnished peroxovanadic solution.

**Preparation of $V_2O_5/TiO_2$ catalyst:** Peroxovanadic solution **(B)** was added to the titanium peroxo-complex solution **(A)** dropwise via droping funnel with continuous stirring to furnish a greenish viscous gel. The resultant gel was dried at 25 $^{o}C$ for 24 h, followed by drying at 80 $^{o}C$ for 12 h and then calcinated at 400 $^{o}C$ for 8 h. The synthesized catalyst was then characterized by using various analytical tools.

**Supplementary Table S1. The calculation for catalyst preparation (for 10 g scale)**

| **Chemical/ Reagents** | **3% (w/w) (C-03)** | **5% (w/w) (C-05)** | **10 %(w/w) (C-10)** | **20%(w/w) (C-20)** | **30%(w/w) (C-30)** |
|---|---|---|---|---|---|
| $Ti(OBu)_4$ | 41.33 g | 40.40 g | 38.35 g | 34.0 g | 29.80 g |
| $H_2O$ | 1000 mL | 1000 mL | 1000 mL | 1000 mL | 1000 mL |
| $H_2O_2$ | 200 mL | 200 mL | 200 mL | 200 mL | 200 mL |
| $TiO_2$ | 9.7 g | 9.5 g | 9.0 g | 8 g | 7.0 g |
| $V_2O_5$ | 0.300 g | 0.500 g | 1.0 g | 2.0 g | 3.0 g |

| | | | | | |
|---|---|---|---|---|---|
| $H_2O$ | 250 mL | 250 mL | 250 mL | 250 mL | 250 mL |
| $H_2O_2$ | 30 mL | 30 mL | 30 mL | 30 mL | 30 mL |

**Characterization of catalyst**

The BET surface area, pore-volume, and pore diameter of the synthesized catalysts (VO@$TiO_2$) were determined by performing nitrogen adsorption and desorption studies. ASAP 2060 (MICROMERITICS, NORCROSS, GA 30 093 USA) instrument is used to determines these properties of the catalyst. Brunauer-Emmett-Teller (BET) equation is used to determine the BET surface area, while the Barrett-Joyner-Halenda (BJH) method is used to estimate the pore size distribution of the catalysts.[1,2] X-ray powder diffraction (XRD) scan of all the prepared catalysts was done with AXS D8-Advance (BRUKER) system, from 2° to 90° angular range to determine the crystalline structure of the catalyst. Fourier-transform infrared spectroscopy (FTIR) of the prepared catalysts was done with Tensor II (BRUKER) instrument in wavenumber ranges from 4000-400 $cm^{-1}$ at room temperature. Ammonia temperature program desorption (TPD- $NH_3$) was done to calculate the acidic sites of the catalyst with the help of ChemiSorb 2750 (MICROMERITICS). Thermogravimetric analysis of catalyst was done by using LINSEIS STA PT1600 thermal analyzer. Approximately 10±1 mg of sample is heated in an alumina crucible from room temperature to 1000 °C under the nitrogen flow of 0.60 L/h.

**Characterization data**

In nitrogen adsorption and desorption studies, nitrogen is adsorbed on the catalyst surface at a cryogenic temperature of −196 °C in the relative pressure range of 0.01-0.9. Fig. S1 shows the $N_2$ adsorption/desorption curve and pore size distribution for the C-10 and C-20 catalysts,[1,2] which demonstrate better results in comparison to others. Also, table S2 summarized the BET surface area, pore-volume, and pore diameter of all the prepared catalysts having a different ratio of vanadium (VO) doped on $TiO_2$ base. Both C-10 and C-20 catalysts follow a similar trend of adsorption/desorption to type-IV IUPAC classification, which confirms the mutual monolayer and multilayer adsorption with capillary condensation.[3] Furthermore, both the catalyst corresponds to the H2 type of hysteresis loop confirms the disordered pores with

**Table S2:** BET surface area, pore-volume, pore size, and average crystallite size and acidic site calculated from data obtained from $NH_3$-TPD of synthesized catalysts

| Sample code | C-03 | C-05 | C-10 | C-20 | C-30 |
|---|---|---|---|---|---|
| BET Surface area ($m^2/g$) | 56.98 | 73.29 | 81.02 | 149.68 | 172.54 |
| Single point adsorption total pore volume ($cm^3/g$) | 0.12 | 0.134 | 0.136 | 0.160 | 1.805 |
| BJH Adsorption pore size (Å) | 78.13 | 73.18 | 67.40 | 42.8 | 35.4 |
| Average crystallite size (Å)* | 94.89 | 97.67 | 124.56 | 119.11 | 108.00 |
| Total acidic sites (mmol/g) | 0.180 | 0.193 | 0.303 | 0.840 | 0.974 |

*Calculated by Scherrer formula

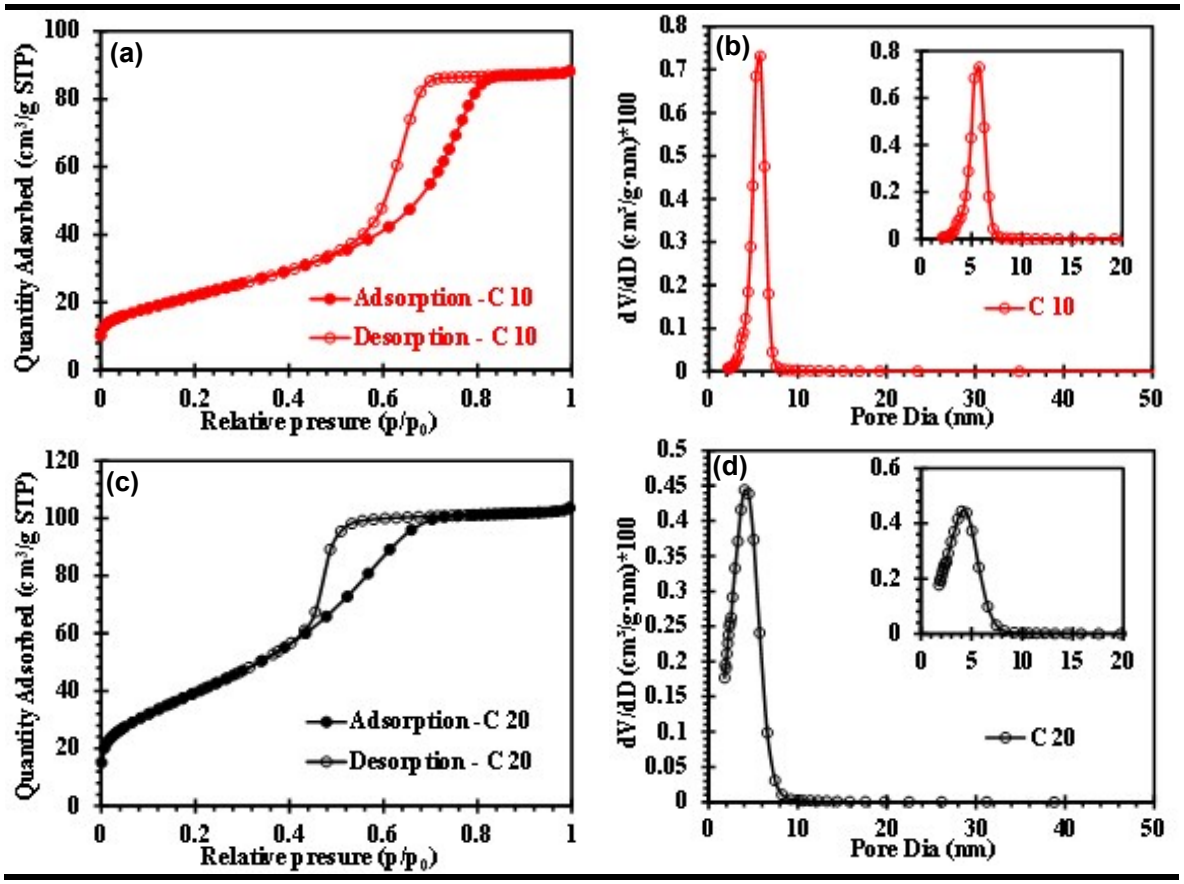


**Fig. S1.** Surface area and porosity

percolation and pore-blocking phenomenon. Fig. S1, b and d show that the catalyst is mesoporous (500 Å < d < 20 Å) in nature as the maximum pore diameters lie between 20-500 Å (instate figures). On increasing the doping ratio of active metal (VO) on support ($TiO_2$) BET surface area increases from 56.98 $m^2/g$ to 172.54 $m^2/g$ for the catalyst C-03 to C-30, respectively. On the other hand, average crystallite size first increases from 94.89 Å to 97.67 Å and 124.56 Å for C-03, C-05, and C-10 respectively, subsequently decreases to 119.11 Å and 108 Å for C-20 and C-30.

The crystalline structure of the catalyst was determined by XRD patterns obtained for all the synthesized catalysts as shown in Fig. S2. Crystalline phases present in the catalyst with different doping ratios of vanadium were matched with anatase-$TiO_2$ (PDF#73-1285) and rutile-$TiO_2$, (PDF#73-2224). The sharp peak of the anatase phase of $TiO_2$ was observed at 29.50° in all catalysts by plane (110), although for the C-10 catalyst, the intensity of peak is maximum. Only $TiO_2$ was traced in two crystalline phases (anatase and rutile) in all the synthesized catalysts having varying intensity. In the C-30 catalyst, the intensity of the peak corresponds to the rutile phase at 32.02° is maximum, which decreases as the impregnation of vanadium increases from 3% to 5%, 10%, 20%, and 30%. This is because, on increasing the active metal impregnation amount, the $TiO_2$ base goes more into the anatase phase rather than the rutile phase.[4] The amount of rutile or anatase phase is highly dependent on the vanadium precursor taken initially for the synthesis of the catalyst.[5] Crystalline phase of vanadium was

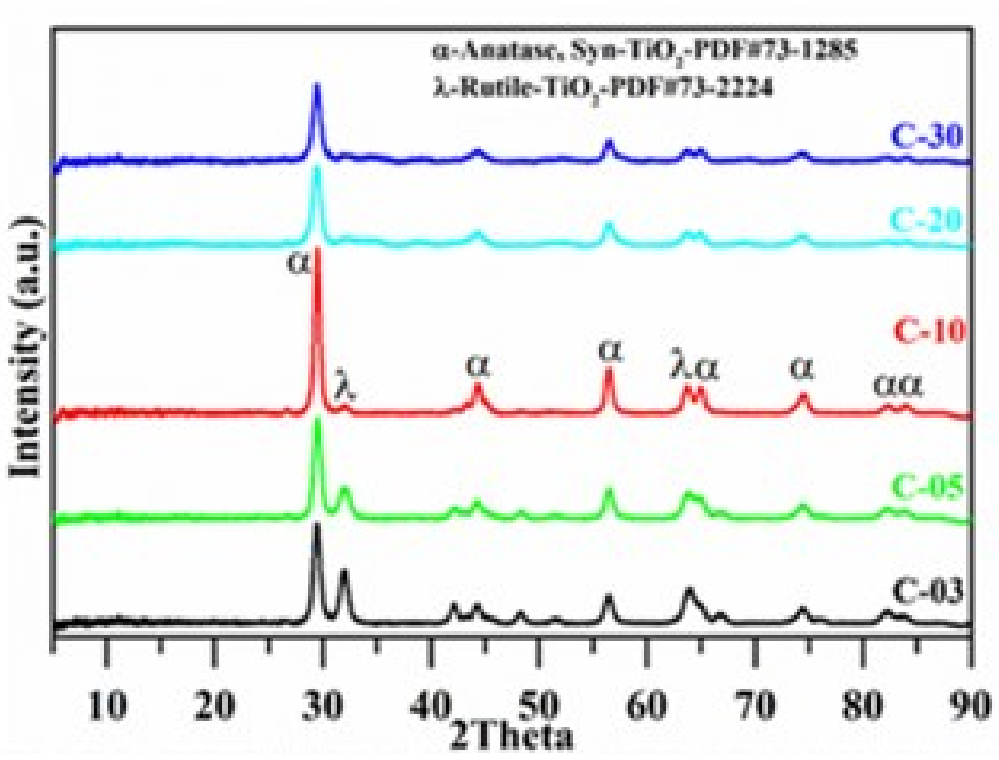


**Fig. S2.** XRD patterns of all the prepared catalysts (C-03, C-05, C-10, C-20, and C-30)

found to be missing may be attributable to hindered nucleation of vanadia particles and gives the conformation that vanadia goes into the dispersed state.[6] Average crystallite size (Å) was calculated by XRD data using the Scherrer formula was tabulated in Table 1.[7] Average crystallite size for 3% vanadia is found to be 94.89 Å, which goes increasing to 124.56 Å for 10%, further increase in vanadia % leads to decreases in crystallite size. The optimum

impregnation was found for the 10% vanadia, on further increasing the amount, the crystalline phase goes demising as the intensity of peaks goes decreasing.

The FT-IR spectra show broadband with maxima around ~3425.84 $cm^{-1}$ which is due to starching vibrations in the hydroxyl group (OH). Peak around ~1620.05 $cm^{-1}$ corresponds to the bending vibration of the $H_2O$ molecules. Peak nearby ~1384.33 $cm^{-1}$ visible in C-03, C-05, and C-10 catalyst is arising due to the Ti-O bond[8,9], which diminished as the vanadia content increases. The peak at ~1020 $cm^{-1}$ and ~820 $cm^{-1}$, which is mainly visible in C-10, C-20, and C-30 were allocated to the lattice vibrations of orthorhombic $V_2O_5$.[10] Furthermore, broadband having maxima at ~690.02 $cm^{-1}$ corresponds to the V-O-V bond (fig. S3).[11]

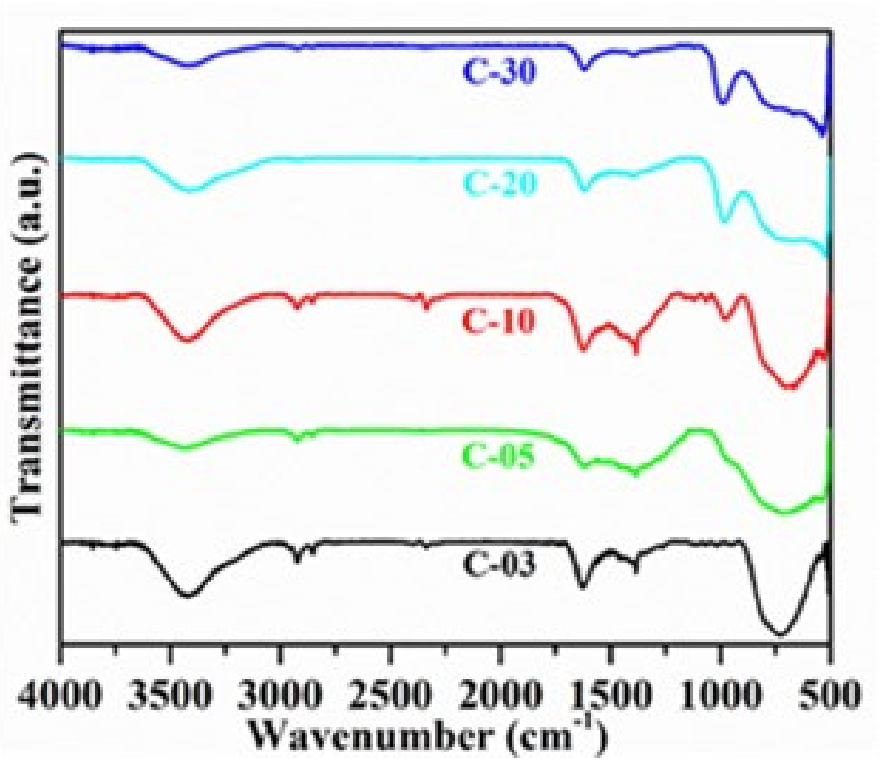


**Fig. S3.** FTIR spectra of catalysts taken at room temperature

The ammonia TPD analysis graph plotted between the TCD signals vs. temperature shows in Fig. S4. Total acidic sites calculated from the ammonia TPD data in mmol/g are shown in table 2. Acidic sites of the catalyst are categorized into week sites (<200 °C), moderate sites (200 °C-450 °C), and strong sites (>450 °C) based on different temperature ranges.[12] Acidic strength of the catalyst increases from 0.193 mmol/g to 0.335 mmol/g on increasing the vanadia impregnation from 3% to 20% on $TiO_2$ support. Although, a further increase in vanadia impregnation to 30% leads to a decrease of acidic strength. Catalysts C-03, C-05, C-10, C-20

and C-30 have total acidity of 0.193, 0.199, 0.303, 0.335 and 0.158 mmol/g respectively (table S3). C-10 shows a high-intensity peak around ~700 °C related to a high Bronsted acid site (fig. S4).[13]

**Table S3:** TPD- $NH_3$ for determining weak, moderate, and strong acidic sites

| **Catalyst** | **TPD analysis of adsorbed $NH_3$ (mmol/g)** | | | |
|---|---|---|---|---|
| | **Weak (<200°C)** | **Moderate (200 °C-450 °C)** | **Strong (>450 °C)** | **Total Acidity (mmol/g)** |
| C-03 | 0.016 | 0.101 | 0.077 | 0.193 |
| C-05 | 0.016 | 0.065 | 0.199 | 0.199 |
| C-10 | 0.011 | 0.034 | 0.258 | 0.303 |
| C-20 | 0.119 | 0.077 | 0.139 | 0.335 |
| C-30 | 0.048 | 0.090 | 0.020 | 0.158 |

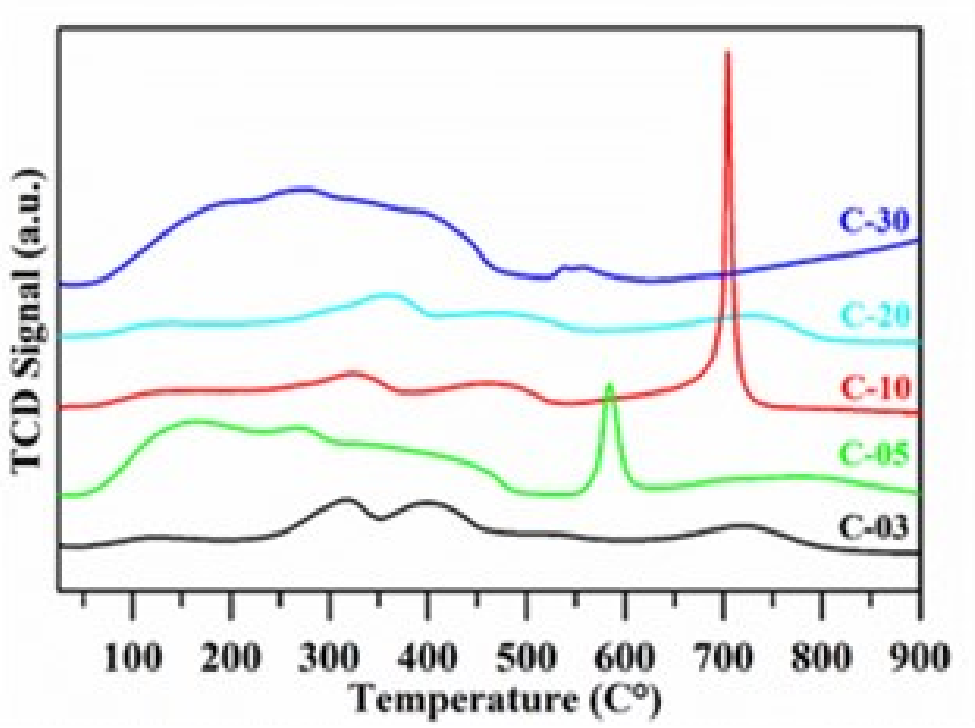


**Fig. S4.** TPD-$NH_3$ of the synthesized catalyst

The thermogravimetric behaviour of C-10 and C-20 catalysts was shown in Fig. S5. C-10 catalyst shows about 10.4% of total weight loss, although the C-20 catalyst shows 11.9%

weight loss. In the first region from room temperature to 200 °C, the physically and chemically bonded moisture is removed, resulting in 3.2% wt. loss in C-10 and 7.3% wt. loss in C-20.[14] In the second region from 200 °C to 600 °C the weight loss may correspond to the escape of ligand water molecules. In the third region, from 600 °C to 775 °C the conversion of anatase $TiO_2$ to the rutile phase takes place, which results in the weight loss of 3.1% and 1.6% in C-10 and C-20 respectively.[15] On further increase in temperature the weight loss is almost constant in both catalysts.

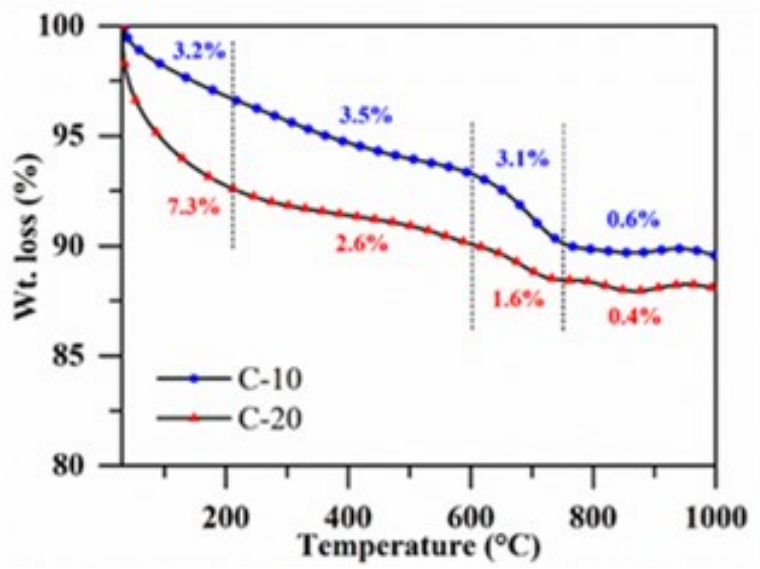


**Fig. S5.** Thermogravimetric analysis of C-10 and C-20 catalyst

**General procedures for VO@$TiO_2$ catalyzed oxidation reactions.**

**General Procedure: (For Styrene oxidation)**

To a screw-capped glass vial charge with styrene derivatives (100.0 mg, 1.0 equiv.) was added 70% aq. TBHP (6.0 equiv.), and C-20 (10 wt. %), the resulting mixture was then stirred at 50° C for 12 h. After completion of the reaction, the catalyst was separated by filtration or by centrifugation methods. The resulting filtrate was then diluted with ethyl acetate and washed with 2N HCl solution and the pooled organic layers were dried over $Na_2SO_4$ and solvent was removed under reduced pressure and residue was purified by silica gel chromatography.

**General Procedure: (For fatty acid oxidation)**

To a screw-capped glass vial charge with free fatty acid (1.0 g) was added 70% aq. TBHP (20 mL), and C-20 (30 wt. %), the resulting mixture was then stirred at 80° C for 12 h. After completion of the reaction, the catalysts were separated by filtration or by centrifugation methods. The resulting filtrate was then concentrated under reduced pressure and residue was

washed with hexane to remove impurities and dried to obtained dicarboxylic acid as a major product.

**General procedure for catalyst recyclability**

On completion of the reaction, the reaction mixture was cooled to 25 °C and diluted with ethyl acetate. The catalyst was then recycled *via* filtration or centrifugation method. The catalyst was then washed with the acetone and dried in the oven at 100 °C for 2 h, and again used for the next cycle of the reaction.

**Table S4. Optimization of reaction conditions[a]**

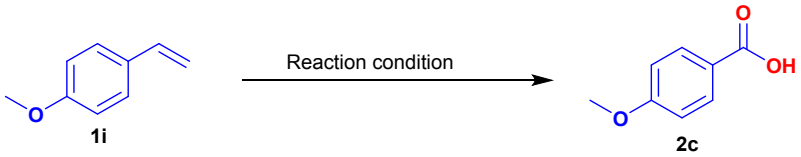

1i 2c

| Entry | Catalyst | Catalyst loading (wt%) | Oxidant | Solvent (1 mL) | Temperature (°C) | Yield[b] (%) |
|---|---|---|---|---|---|---|
| 1 | $CrO_3$ | 10 | TBHP (10 eq.) | ACN | 50 | ND |
| 2 | $ZrO_2$ | 10 | TBHP (10 eq.) | ACN | 50 | ND |
| 3 | $V_2O_5$ | 10 | TBHP (10 eq.) | ACN | 50 | ND |
| 4 | $TiO_2$ | 10 | TBHP (10 eq.) | ACN | 50 | ND |
| 5 | C-05 | 10 | TBHP (10 eq.) | ACN | 50 | ND |
| 6 | C-10 | 10 | TBHP (10 eq.) | ACN | 50 | 50 |
| 7 | C-20 | 10 | TBHP (10 eq.) | ACN | 50 | 72 |
| 8 | C-20 | 10 | TBHP (10 eq.) | DCM | 50 | Trace |
| 9 | C-20 | 10 | TBHP (10 eq.) | EtOAc | 50 | Trace |
| 10 | C-20 | 10 | TBHP (5 eq.) | ACN | 50 | 60 |
| 11 | C-20 | 10 | TBHP (6 eq.) | ACN | 50 | 70 |
| **12** | **C-20** | **10** | **TBHP (6 eq.)** | **-** | **50** | **88** |
| 13 | C-20 | 10 | TBHP (6 eq.) | - | 80 | 86 |
| 14 | C-20 | 10 | TBHP (6 eq.) | - | 25 | 45 |
| 15 | C-20 | 10 | $H_2O_2$ (6 eq.) | - | 50 | 70 |
| 16 | C-20 | 5 | TBHP (6 eq.) | | 50 | 48 |
| 17 | C-20 | 10 | - | - | 50 | ND |
| 18 | - | - | TBHP (6 eq.) | - | 50 | Trace |

[a]Reaction condition: 4-methoxy styrene (1.0 equiv., 50.0 mg), C-20 (10 wt%), TBHP (6.0 equiv.), 50 °C, 12 h, [b]Isolated yield. ND = Not Detected

**Table S5: Optimization of reaction condition for fatty acid oxidation[a]**

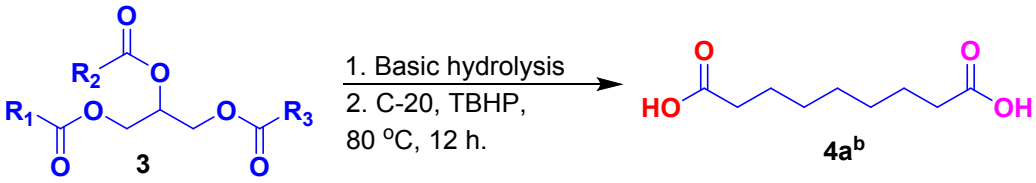


| Entry | FFAs (mg) | TBHP (mL) | Catalyst (C-20) | Time (h) | Temperature (°C) | Conversion (GC %) |
|---|---|---|---|---|---|---|
| 1 | 250 | 1.5 | 75 mg | 12 | 50 | 15 |
| 2 | 250 | 1.5 | 75 mg | 12 | 80 | 29 |
| 3 | 250 | 2.0 | 75 mg | 12 | 80 | 48 |
| 4 | 250 | 3.0 | 75 mg | 12 | 80 | 52 |
| 5 | 250 | 4.0 | 75 mg | 12 | 80 | 56 |
| **6** | **250** | **5.0** | **75 mg** | **12** | **80** | **58** |
| 7 | 250 | 6.0 | 75 mg | 12 | 80 | 55 |
| 8 | 250 | 5.0 | 75 mg | 12 | 100 | 55 |

[a]Reaction condition: FFAs (250.0 mg), C-20 (30 wt%), TBHP (20 Volume), 80 °C, 12 h, [b]GC conversion measured by derivatization of crude reaction mixture to methyl ester.

**Benzoic acid (2a)[16]**

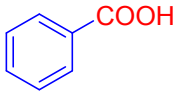


**$^1$H NMR (600 MHz, Chloroform-*d*):** $\delta$ 8.15 (d, $J$ = 7.8 Hz, 2H), 7.64 (t, $J$ = 7.2 Hz, 1H), 7.51 (t, $J$ = 7.2 Hz, 2H). **$^{13}$C NMR (151 MHz, Chloroform-*d*):** $\delta$ 172.3, 133.8, 130.2, 129.3, 128.5.

**4-(*tert*-butyl)benzoic acid (2b)[16]**

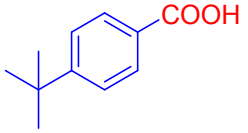


**$^1$H NMR (300 MHz, Chloroform-*d*):** $\delta$ 8.08 (d, $J$ = 8.4 Hz, 2H), 7.52 (d, $J$ = 8.4 Hz, 2H), 1.38 (s, 9H). **$^{13}$C NMR (75 MHz, Chloroform-*d*):** $\delta$ 172.3, 157.6, 130.1, 126.6, 125.5, 35.2, 31.1.

**2,4-dimethylbenzoic acid (2c)[17]**

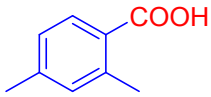


**$^1$H NMR (600 MHz, Methanol-$d_4$):** $\delta$ 7.81 (d, $J$ = 7.8 Hz, 1H), 7.08 (s, 1H), 7.06 (d, $J$ = 7.8 Hz, 1H), 2.54 (s, 3H), 2.34 (s, 3H). **$^{13}$C NMR (151 MHz, Methanol-$d_4$):** $\delta$ 171.1, 143.8, 141.4, 133.4, 132.1, 128.3, 127.4, 21.9, 21.3.

**4-methoxybenzoic acid (2d)[16]**

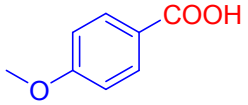


**$^1$H NMR (300 MHz, Chloroform-*d*):** $\delta$ 8.09 (d, $J$ = 8.9 Hz, 2H), 6.97 (d, $J$ = 8.9 Hz, 2H), 3.90 (s, 3H). **$^{13}$C NMR (75 MHz, Chloroform-*d*):** $\delta$ 171.5, 164.1, 132.4, 121.7, 113.8, 55.5.

**2,4-dimethoxybenzoic acid (2e)[18]**

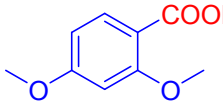


**$^1$H NMR (300 MHz, DMSO-$d_6$):** $\delta$ 12.15 (s, 1H), 7.72-7.68 (m, 1H), 6.62-6.54 (m, 2H), 3.82 (s, 6H). **$^{13}$C NMR (75 MHz, Chloroform-*d*):** $\delta$ 166.3, 163.6, 160.6, 133.2, 112.6, 105.1, 98.8, 55.7, 55.4.

**4-acetoxybenzoic acid (2f)[16]**

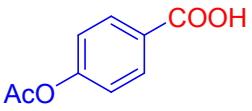


**$^1$H NMR (300 MHz, Chloroform-*d*):** $\delta$ 8.17 (d, $J$ = 8.7 Hz, 2H), 7.24 (d, $J$ = 8.7 Hz, 2H), 2.36 (s, 3H). **$^{13}$C NMR (75 MHz, Chloroform-*d*):** $\delta$ 171.2, 168.8, 155.0, 131.9, 126.8, 121.7, 21.1.

**4-chlorobenzoic acid (2g)[18]**

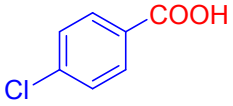


**$^1$H NMR (300 MHz, DMSO-$d_6$):** $\delta$ 13.17 (s, 1H), 7.94 (d, $J$ = 8.6 Hz, 2H), 7.56 (d, $J$ = 8.5 Hz, 2H). **$^{13}$C NMR (75 MHz, Chloroform-*d*)**: $\delta$ 166.4, 137.7, 131.1, 129.6, 128.7.

**4-bromobenzoic acid (2h)[16]**

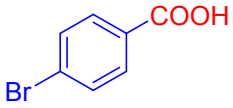


**$^1$H NMR (300 MHz, DMSO-$d_6$):** $\delta$ 7.88-7.83 (m, 2H), 7.74-7.64 (m, 2H). **$^{13}$C NMR (75 MHz, Chloroform-*d*):** $\delta$ 166.6, 131.60, 131.24, 130.3, 126.7.

**3-nitrobenzoic acid (2i)[19]**

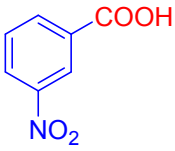


**$^1$H NMR (300 MHz, DMSO-$d_6$):** $\delta$ 8.61-8.60 (m, 1H), 8.48-8.43 (m, $J$ = 8.5, 2.7 Hz, 1H), 8.36-8.31 (m, 1H), 7.84-8.77 (m, 1H). **$^{13}$C NMR (75 MHz, $CDCl_3$):** $\delta$ 165.5, 147.9, 135.3, 132.5, 130.5, 127.2, 123.6.

**[1,1'-biphenyl]-4-carboxylic acid (2j)[20]**

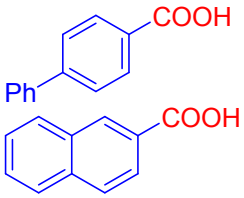


**$^1$H NMR (300 MHz, DMSO-$d_6$):** $\delta$ 8.04-7.99 (m, 2H), 7.81-7.70 (m, 4H), 7.53-7.41 (m, 3H). **$^{13}$C NMR (75 MHz, $CDCl_3$):** $\delta$ 167.1, 144.3, 139.0, 129.9, 129.6, 129.0, 128.2, 126.9, 126.8.

**2-naphthoic acid (2k)[18]**

**$^1$H NMR (300 MHz, DMSO-$d_6$):** $\delta$ 8.60 (s, 1H), 8.11 (d, $J$ = 7.9 Hz, 1H), 8.03-7.95 (m, 3H), 7.67-7.57 (m, 2H). **$^{13}$C NMR (75 MHz, $CDCl_3$):** $\delta$ 167.4, 134.9, 132.1, 130.5, 129.2, 128.3, 128.1, 128.0, 127.6, 126.8, 125.1.

**Acetophenone (2l)[16]**

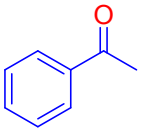


**$^1$H NMR (600 MHz, Chloroform-*d*):** $\delta$ 7.98 (d, $J$ = 8.4 Hz, 2H), 7.58 (t, $J$ = 7.8 Hz, 1H), 7.48 (t, $J$ = 7.8 Hz, 2H), 2.62 (s, 3H). **$^{13}$C NMR (151 MHz, Chloroform-*d*):** $\delta$ 198.1, 137.1, 133.1, 128.5, 128.3, 26.6.

**4-((2-methoxy-2-oxoethyl)carbamoyl)benzoic acid (2m)**

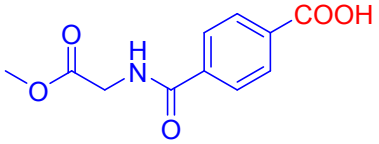


**$^1$H NMR (600 MHz, DMSO-$d_6$):** $\delta$ 13.23 (s, 1H), 9.14 (t, $J$ = 6.0 Hz, 1H), 8.04 (d, $J$ = 8.4 Hz, 2H), 7.96 (d, $J$ = 8.4 Hz, 2H), 4.03 (d, $J$ = 6.0 Hz, 2H), 3.66 (s, 3H). **$^{13}$C NMR (151 MHz, DMSO-$d_6$):** $\delta$ 170.2, 166.7, 165.9, 137.3, 133.3, 129.3, 127.5, 51.8, 41.2. HRMS (ESI): m/z calc'd for $C_{12}H_{54}O_4$ $[M+H]^+$ : 551.4095, found : 551.4098

**(S)-4-((1-methoxy-1-oxopropan-2-yl)carbamoyl)benzoic acid (2n)**

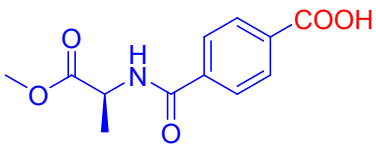


**$^{1}$H NMR (600 MHz, DMSO-$d_6$):** $\delta$ 13.22 (s, 1H), 8.98 (d, $J$ = 6.6 Hz, 1H), 8.03 (d, $J$ = 8.4 Hz, 2H), 7.97 (d, $J$ = 8.4 Hz, 2H), 4.52 – 4.47 (m, 1H), 3.65 (s, 3H), 1.41 (d, $J$ = 7.2 Hz, 3H). **$^{13}$C NMR (151 MHz, DMSO-$d_6$):** $\delta$ 173.4, 167.1, 165.9, 137.8, 133.6, 129.6, 128.1, 52.3, 48.7, 17.1. HRMS (ESI): m/z calc′d for $C_{11}H_{11}NO_5$ $[M+H]^+$ : 238.0710, found : 238.0710.

**Azelaic acid (4a)[21]**

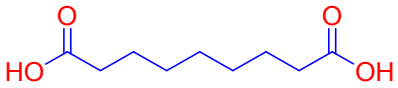


**$^{1}$H NMR (600 MHz, DMSO-$d_6$):** $\delta$ 2.16 (t, $J$ = 7.2 Hz, 4H), 1.46-1.42 (m, 4H), 1.21 (s, 6H). **$^{13}$C NMR (151 MHz, DMSO-$d_6$):** $\delta$ 175.2, 34.0, 28.7, 24.8.

## Benzoic acid (2a)

### $^{1}H_{1}$ NMR

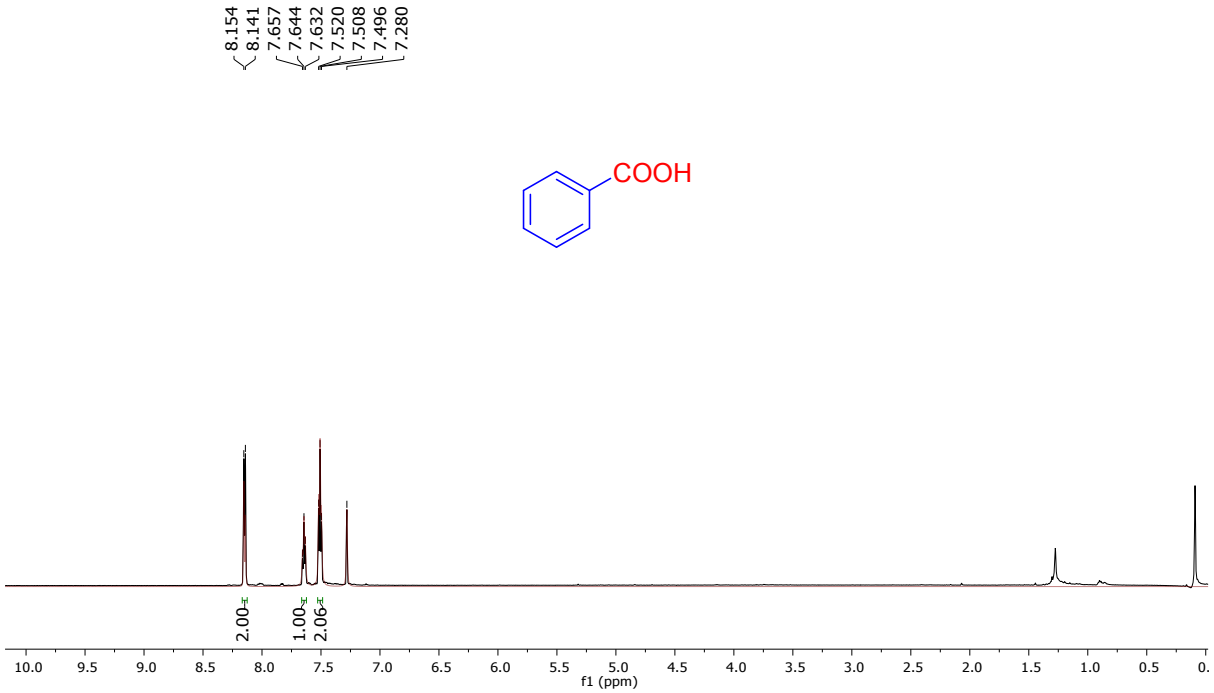


### $^{13}C$ NMR

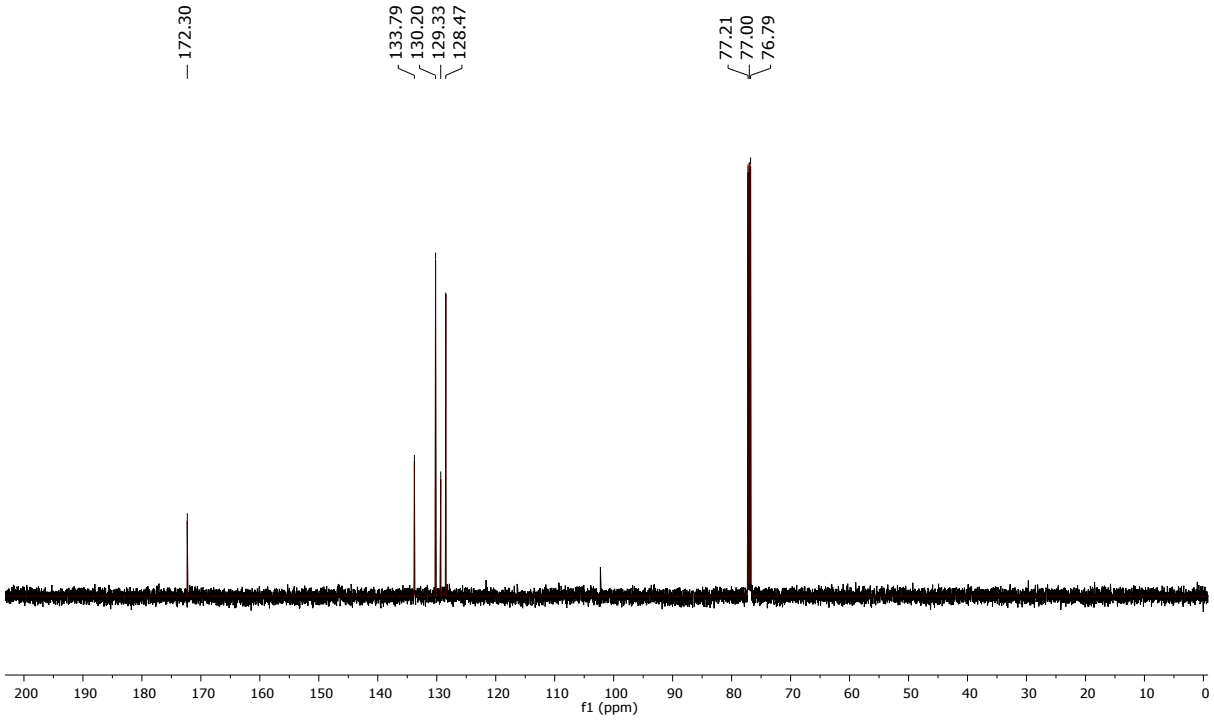

## 4-(*tert*-butyl)benzoic acid (2b)

### $^{1}H_{1}$ NMR

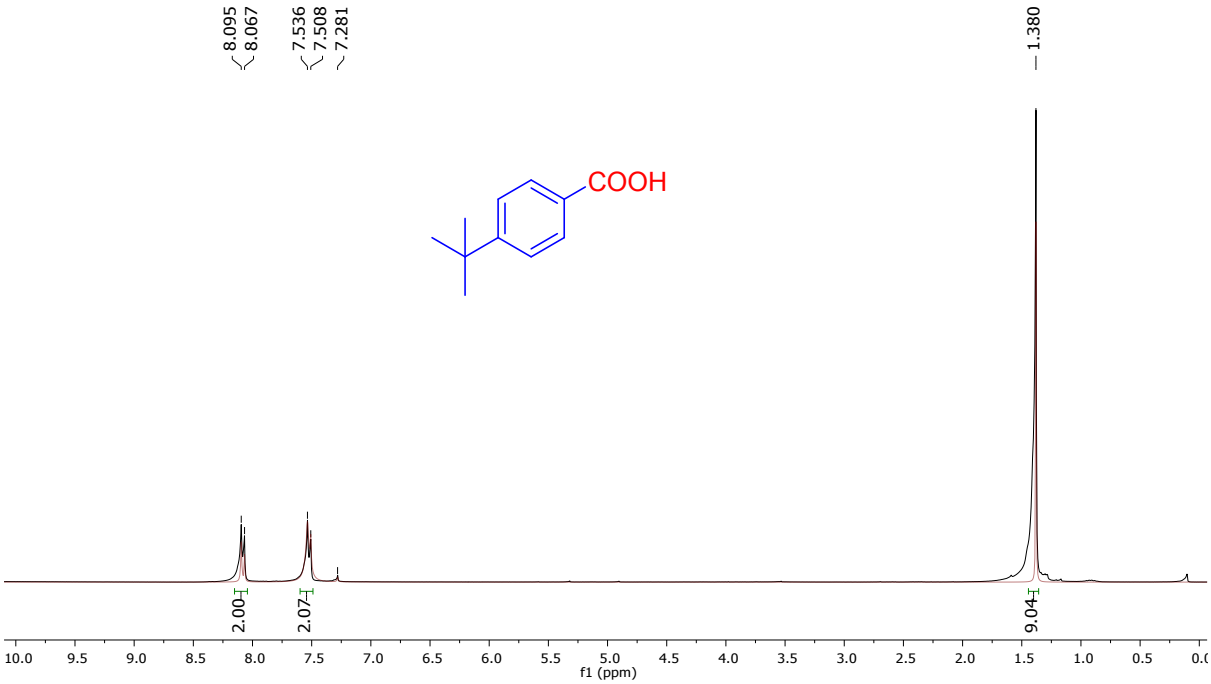


### $^{13}C$ NMR

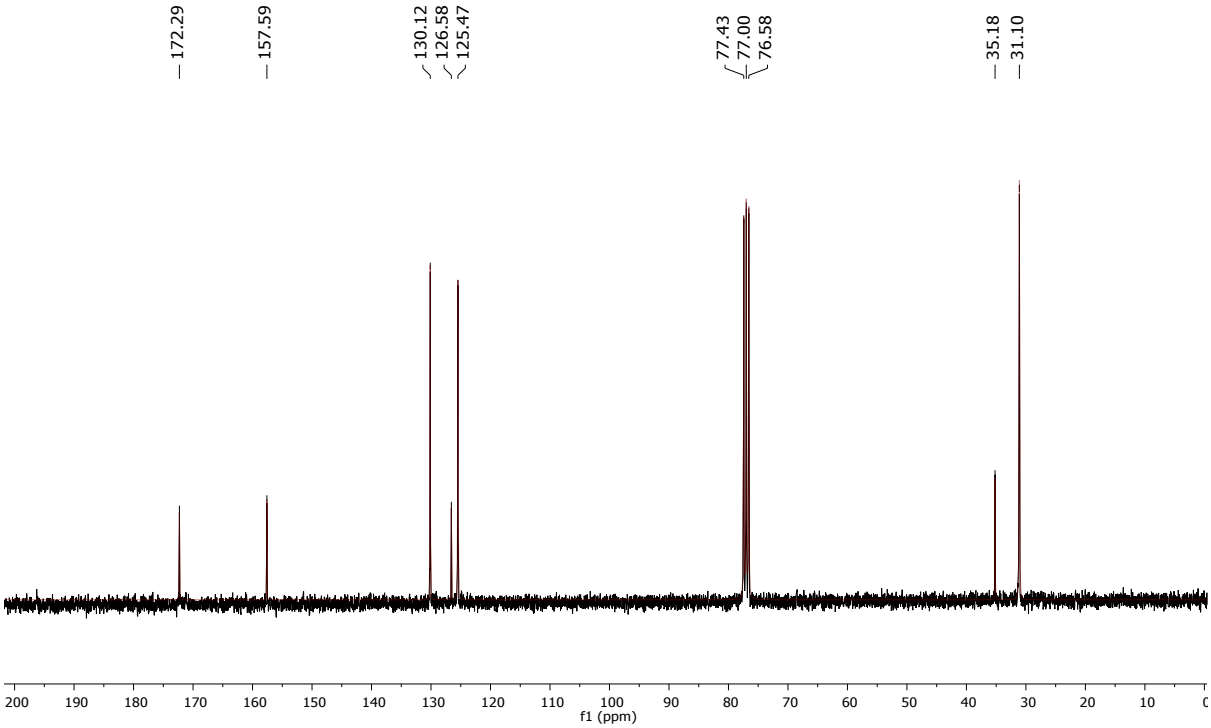

## 2,4-dimethylbenzoic acid (2c)

### $^{1}H_{1}$ NMR

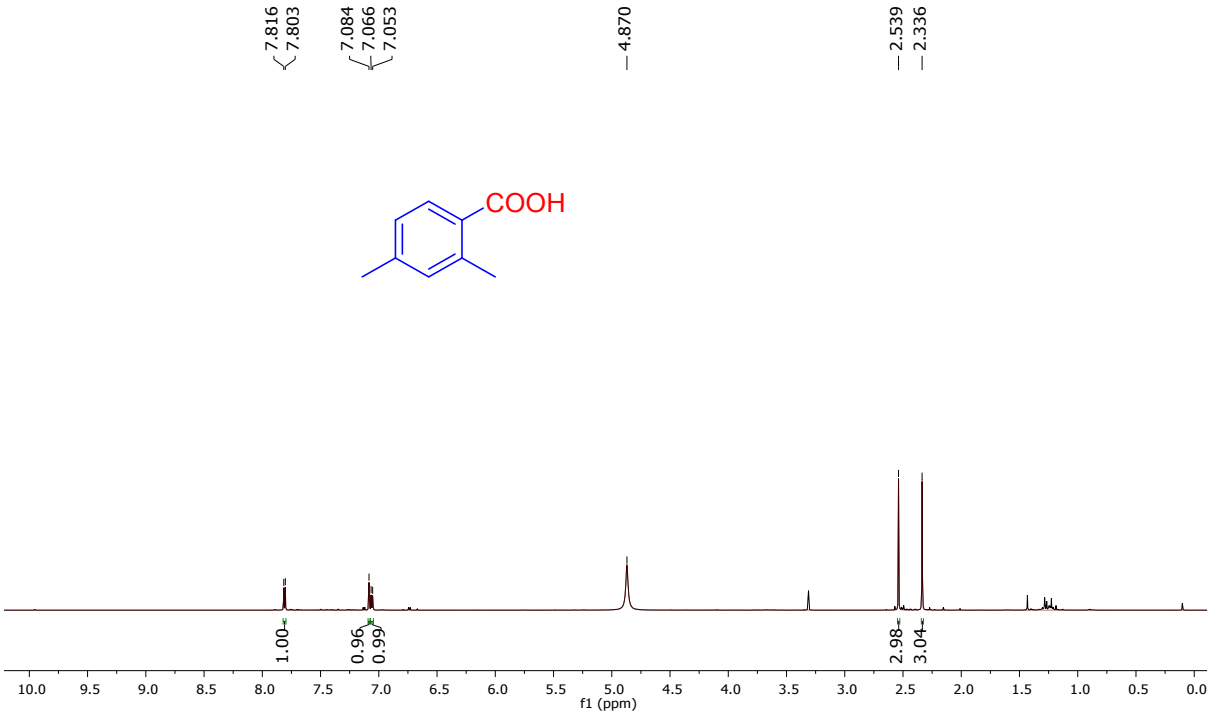


### $^{13}C$ NMR

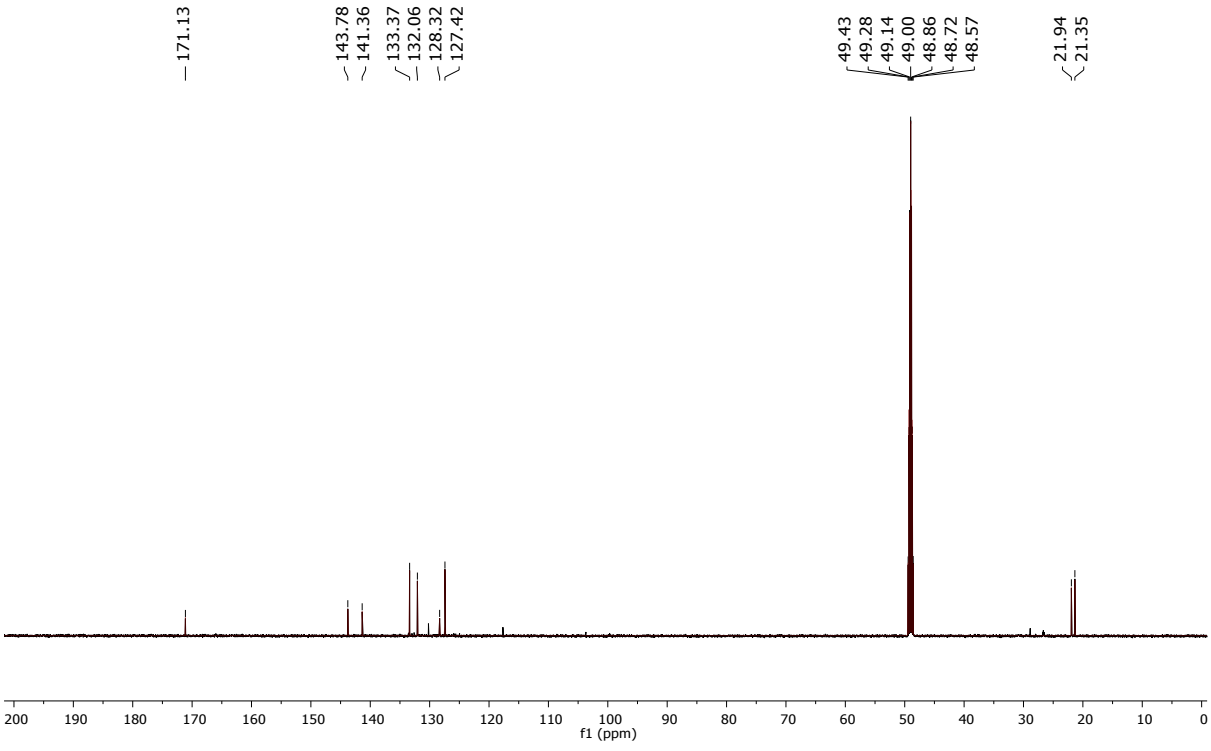

## 4-methoxybenzoic acid (2d)

### $^{1}H_{1}$ NMR

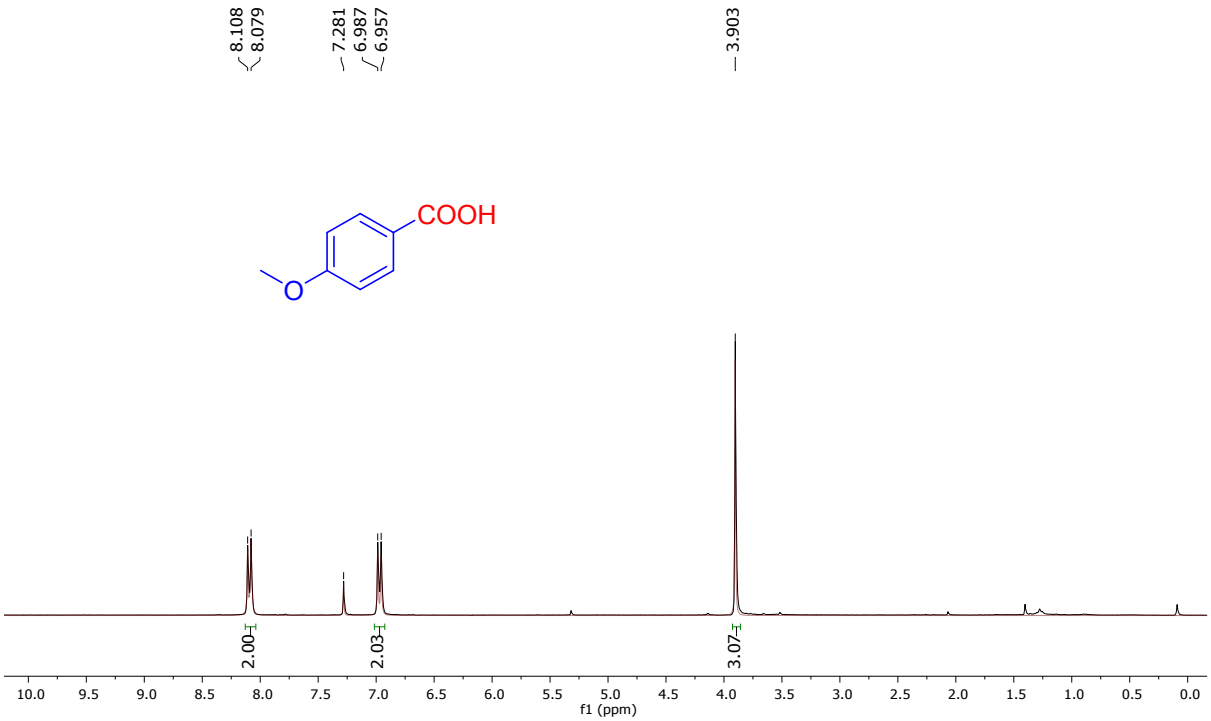


### $^{13}C$ NMR

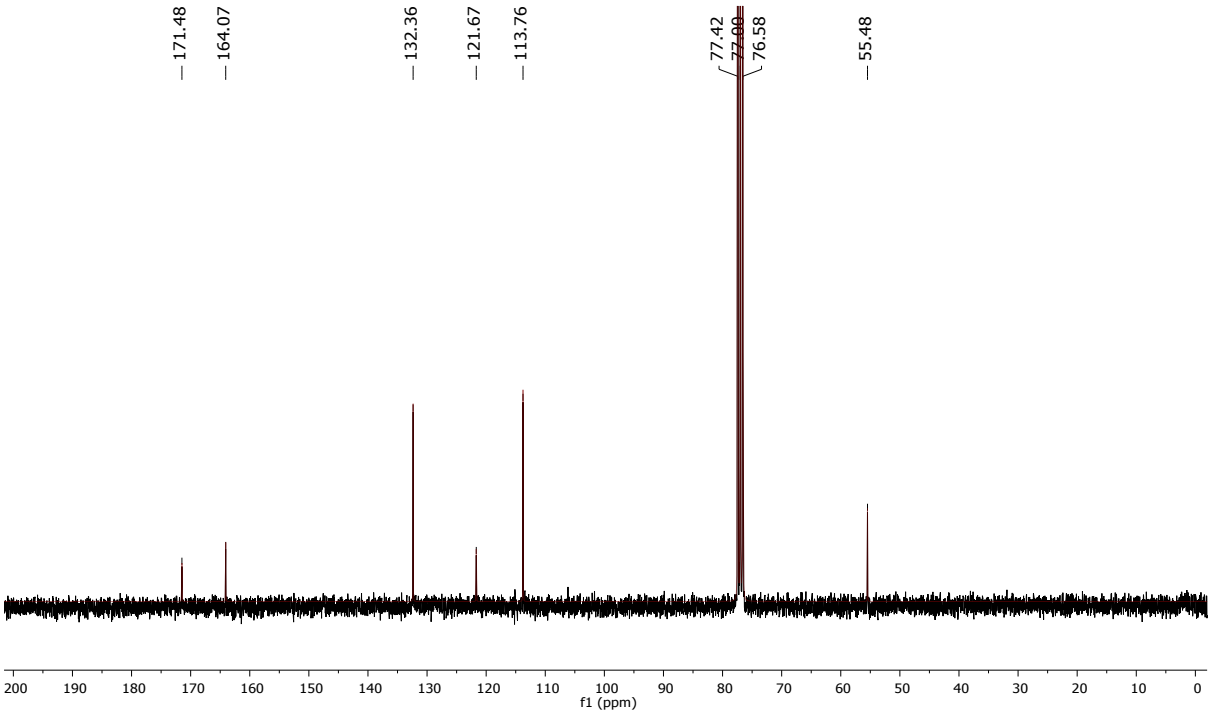

## 2,4-dimethoxybenzoic acid (2e)

### $^{1}H_{1}$ NMR

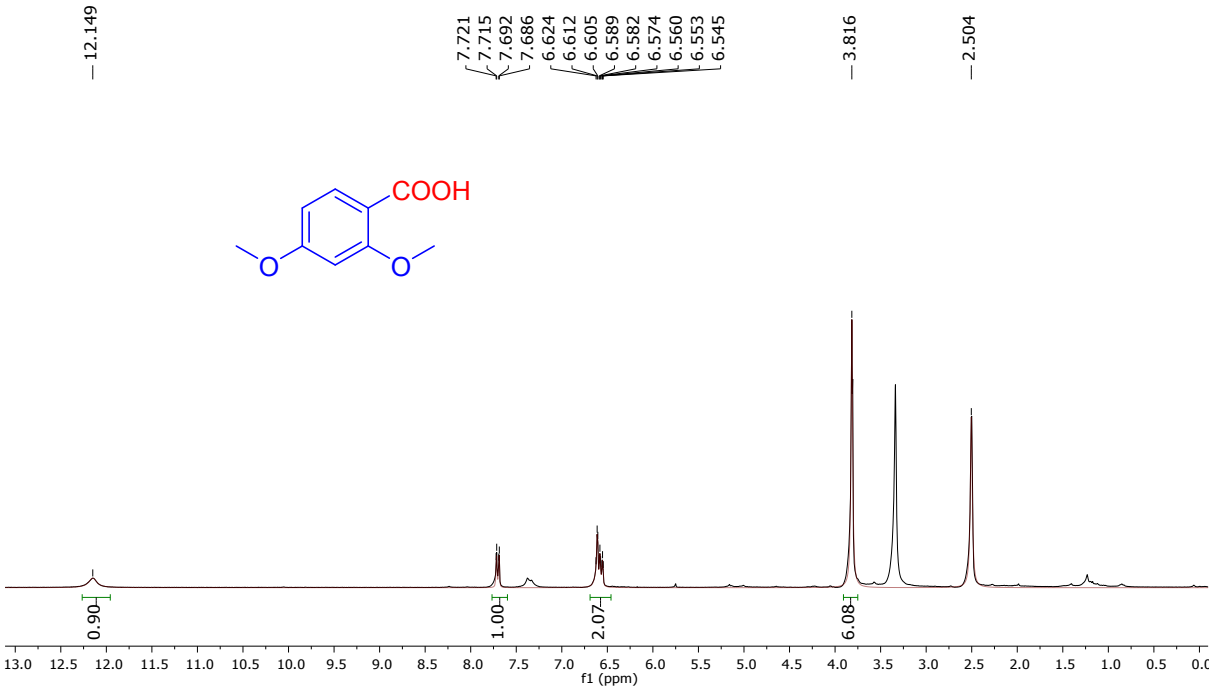


### $^{13}C$ NMR

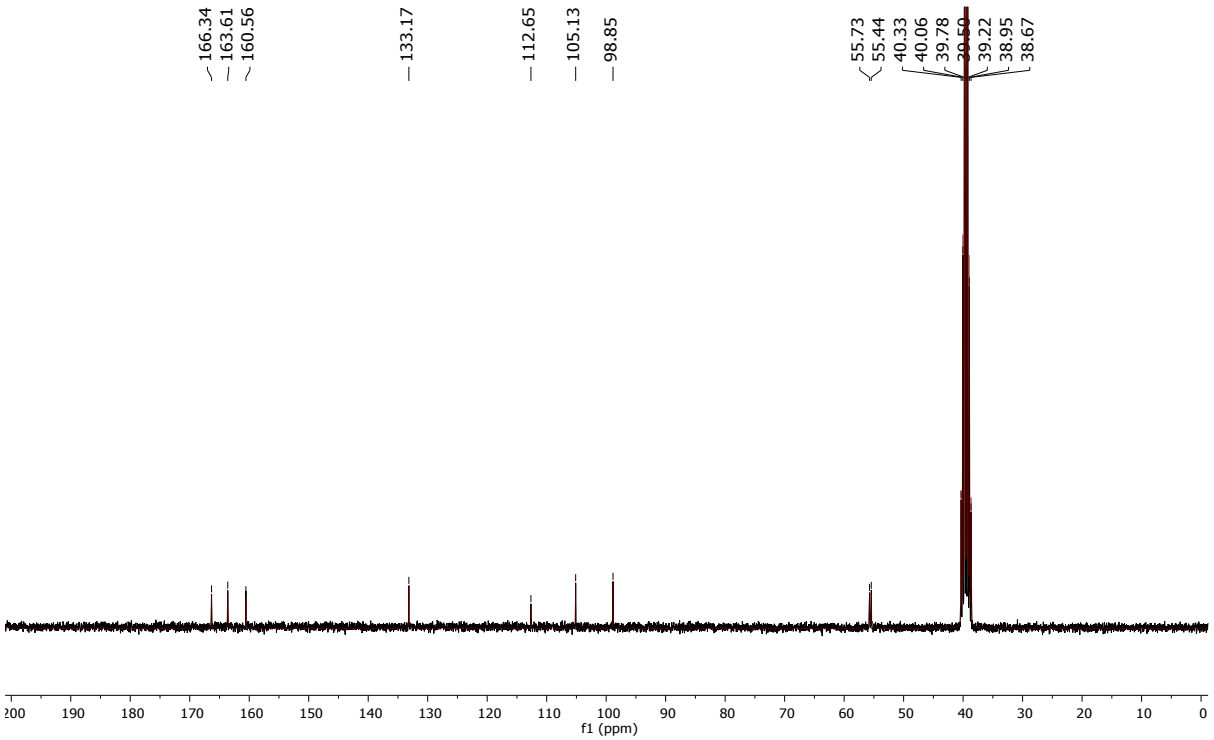

## 4-acetoxybenzoic acid (2f)

### $^{1}H_{1}$ NMR

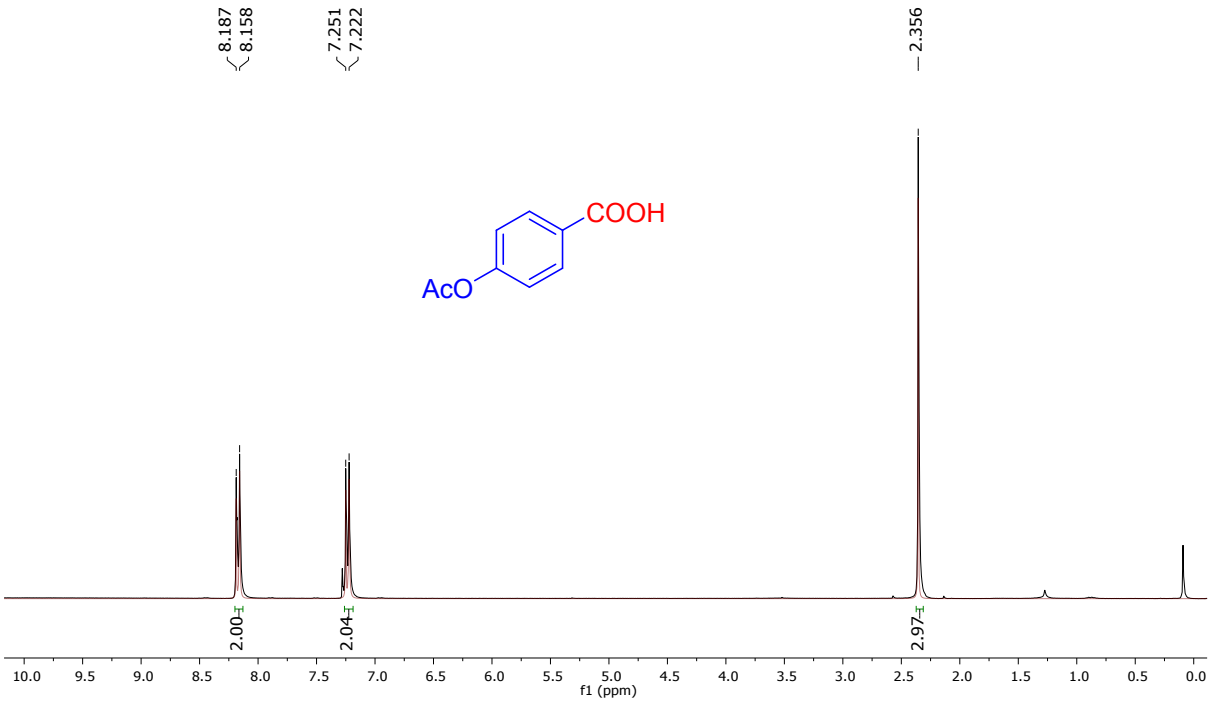


### $^{13}C$ NMR

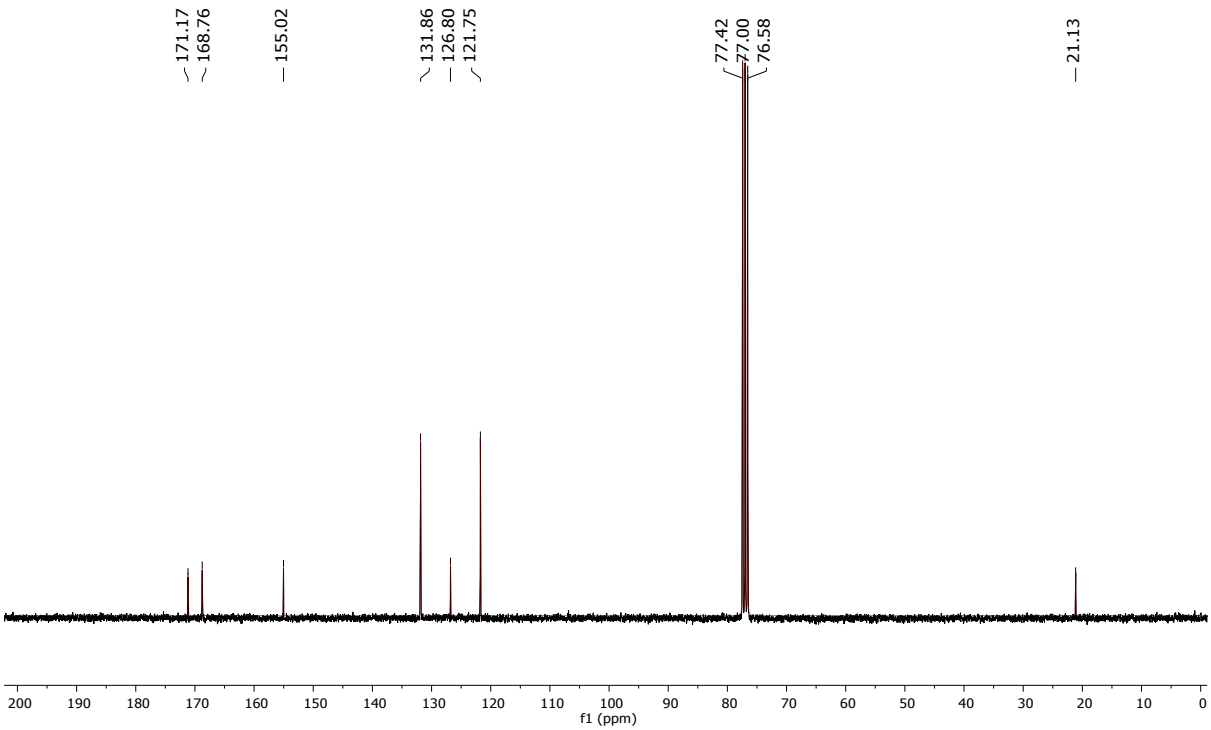


## 4-chlorobenzoic acid (2g)

## $^{1}H_{1}$ NMR

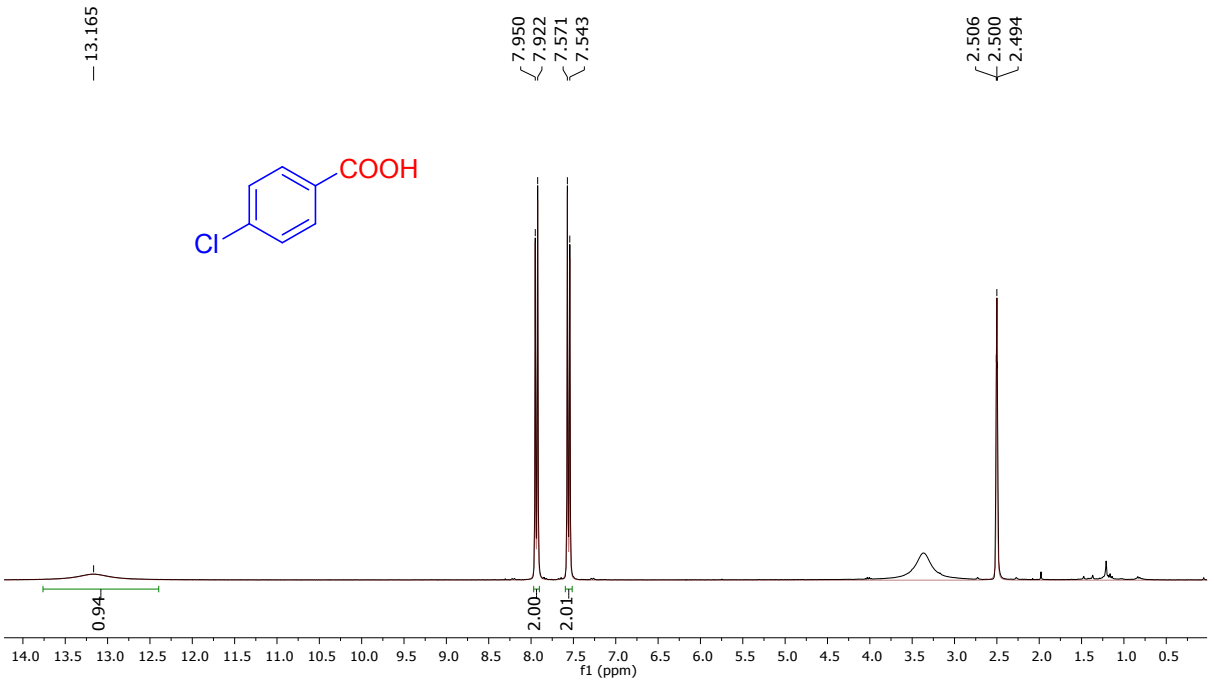


## $^{13}C$ NMR

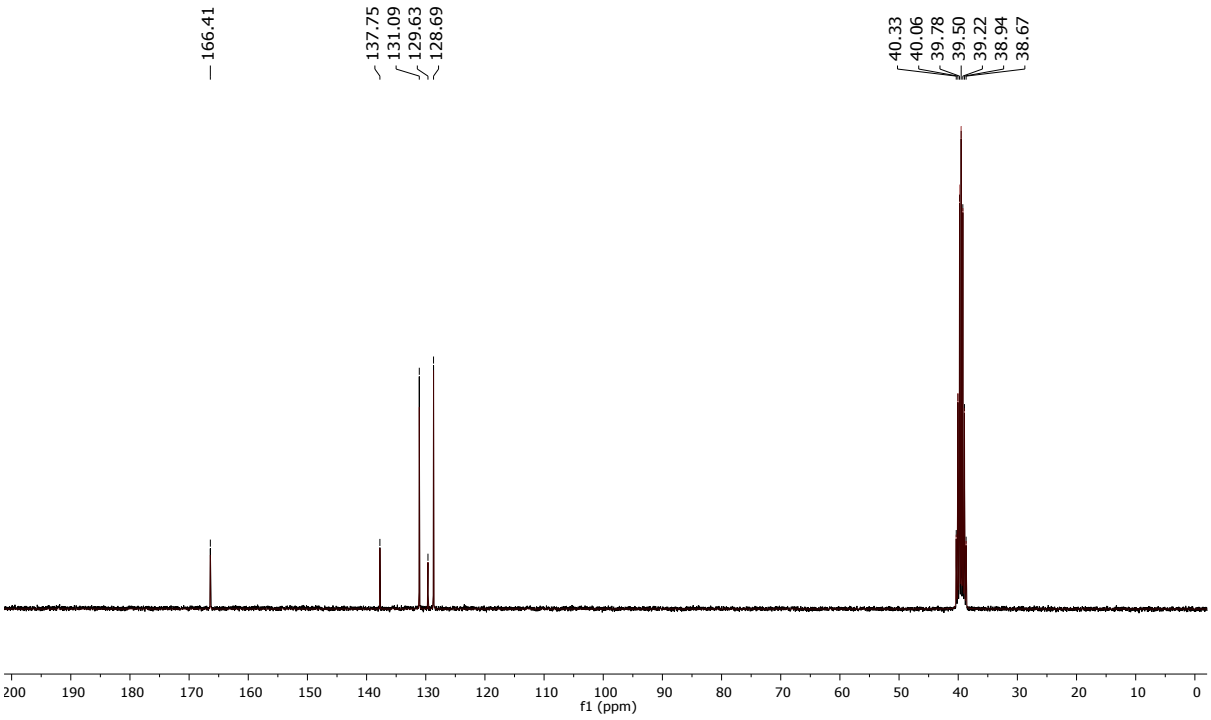


## 4-bromobenzoic acid (2h)

## $^{1}H_{1}$ NMR

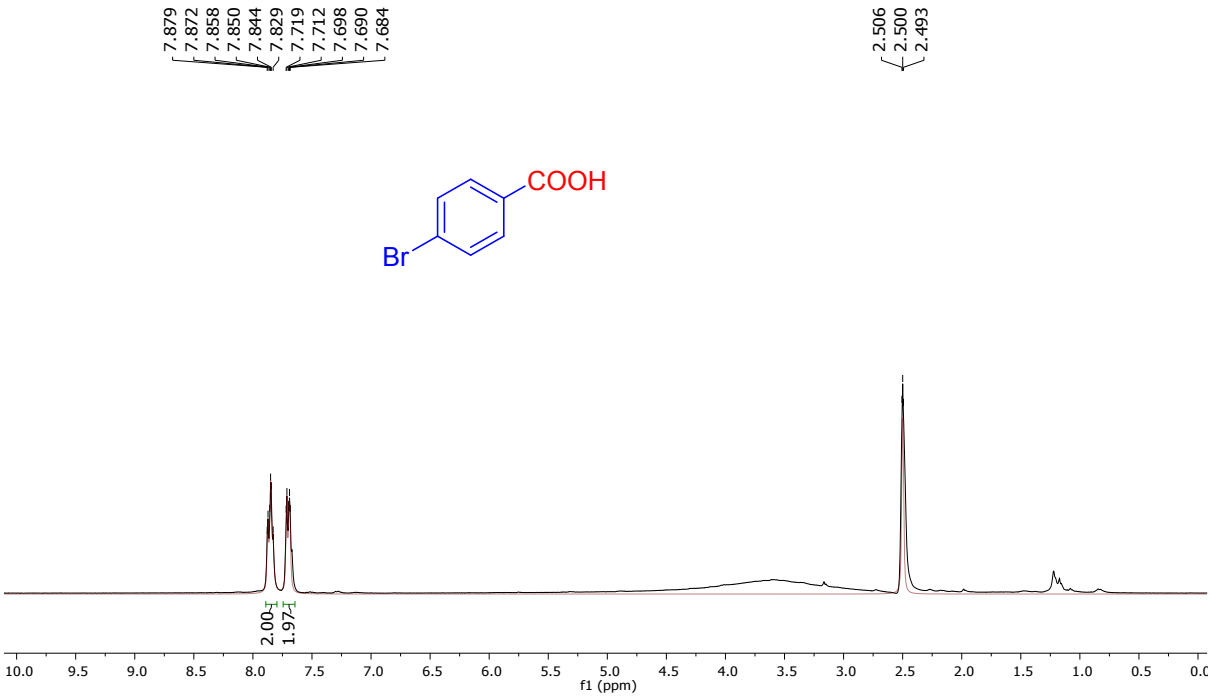


## $^{13}C$ NMR

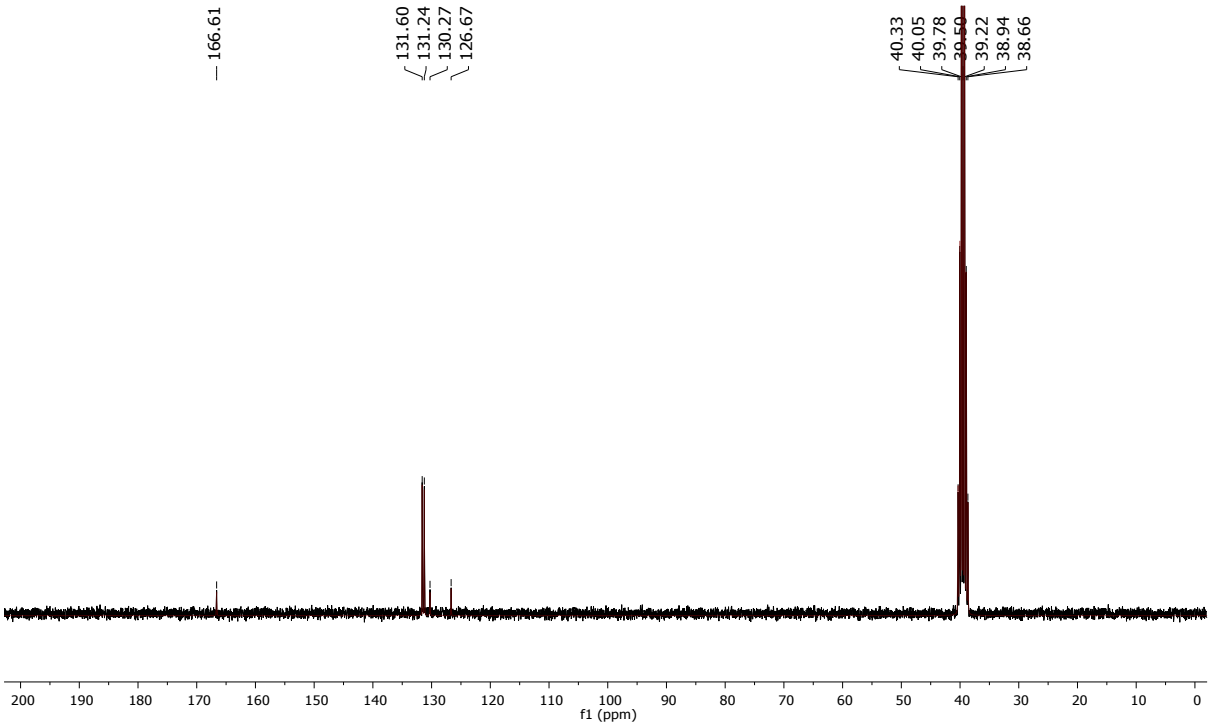


## 3-nitrobenzoic acid (2i)

## $^{1}H_{1}$ NMR

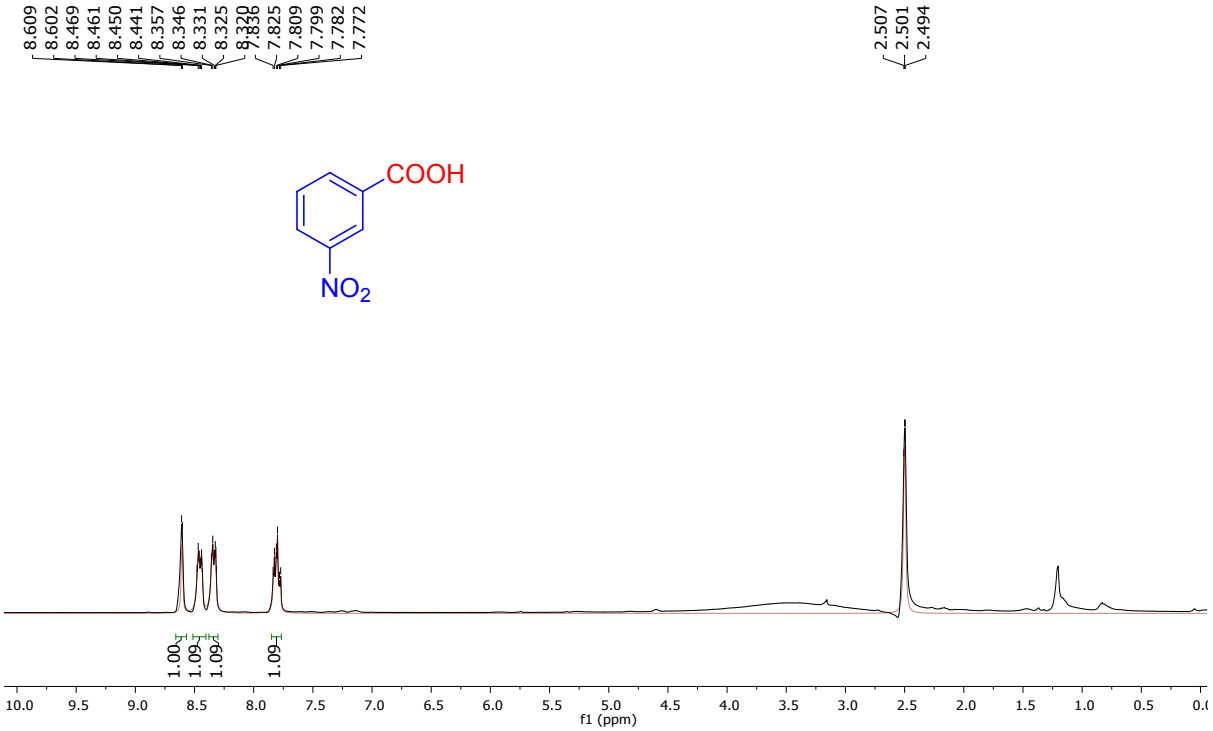


## $^{13}C$ NMR

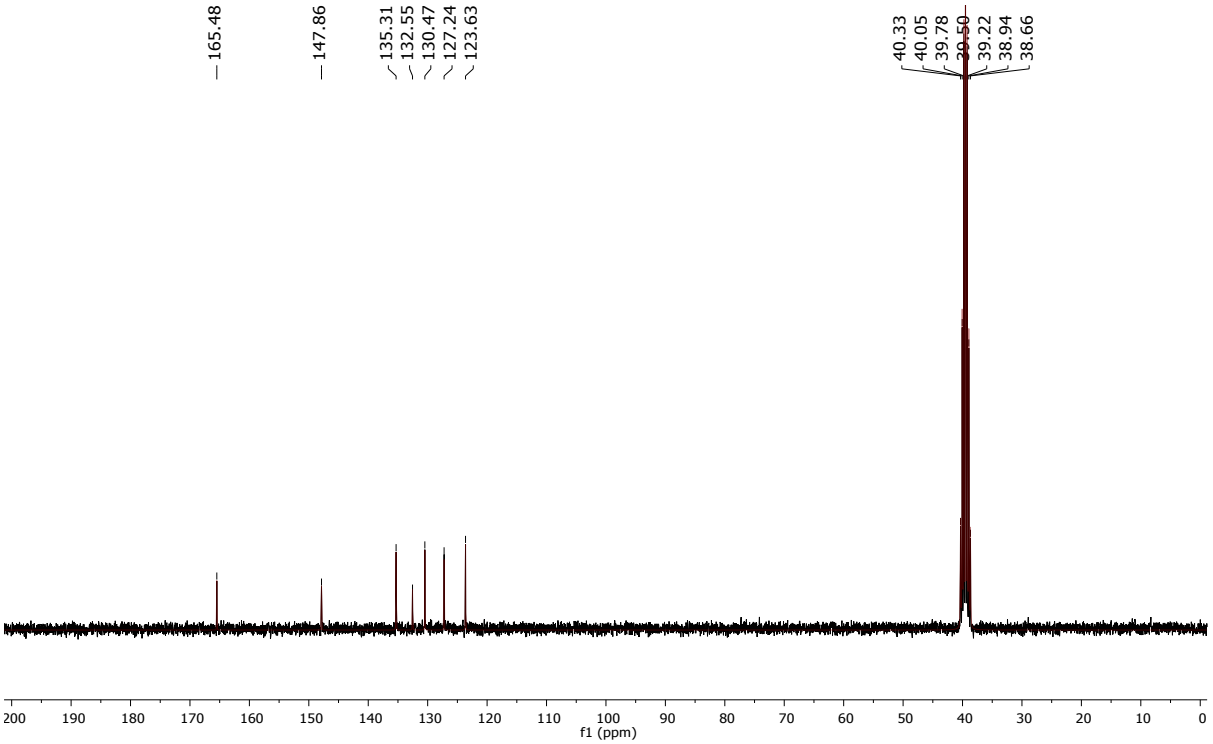


**[1,1'-biphenyl]-4-carboxylic acid (2j)**

## $^{1}$H NMR

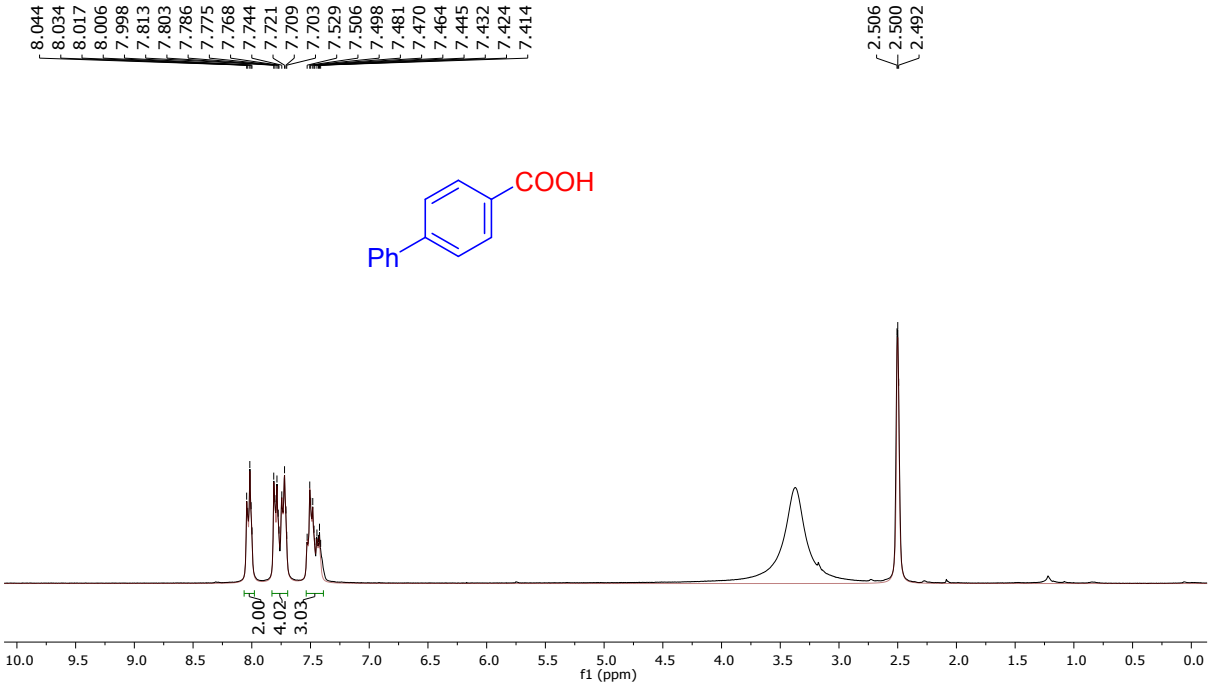


## $^{13}$C NMR

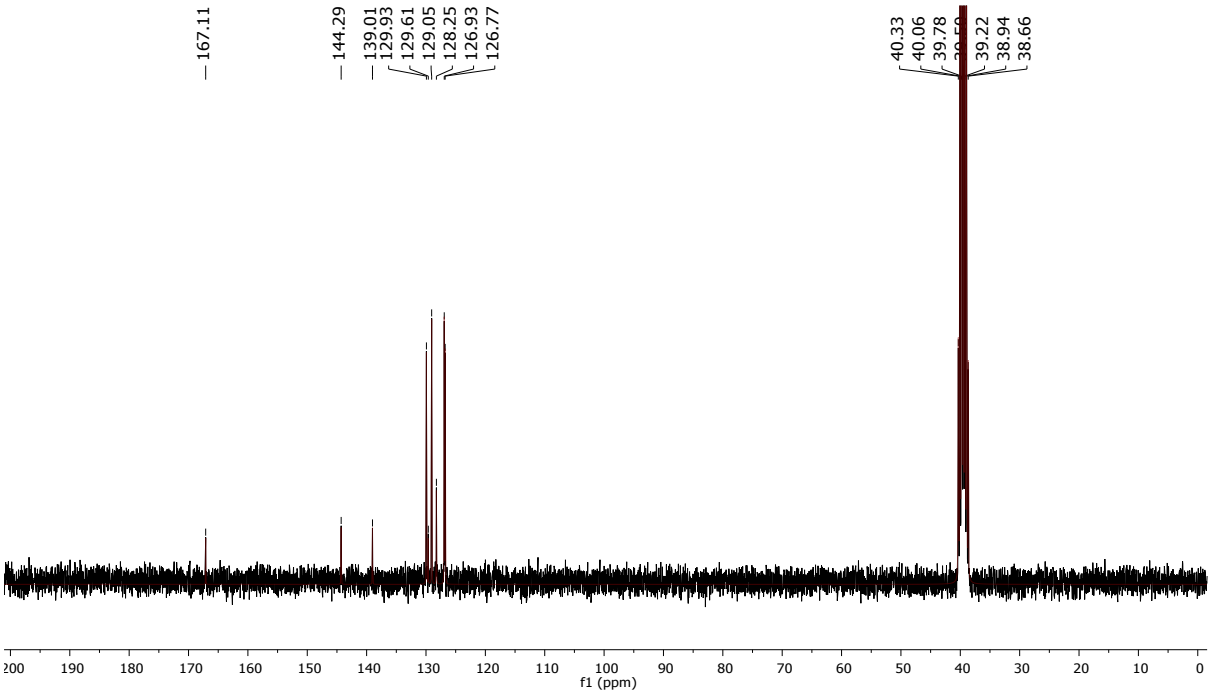


## 2-naphthoic acid (2k)

## $^{1}$H NMR

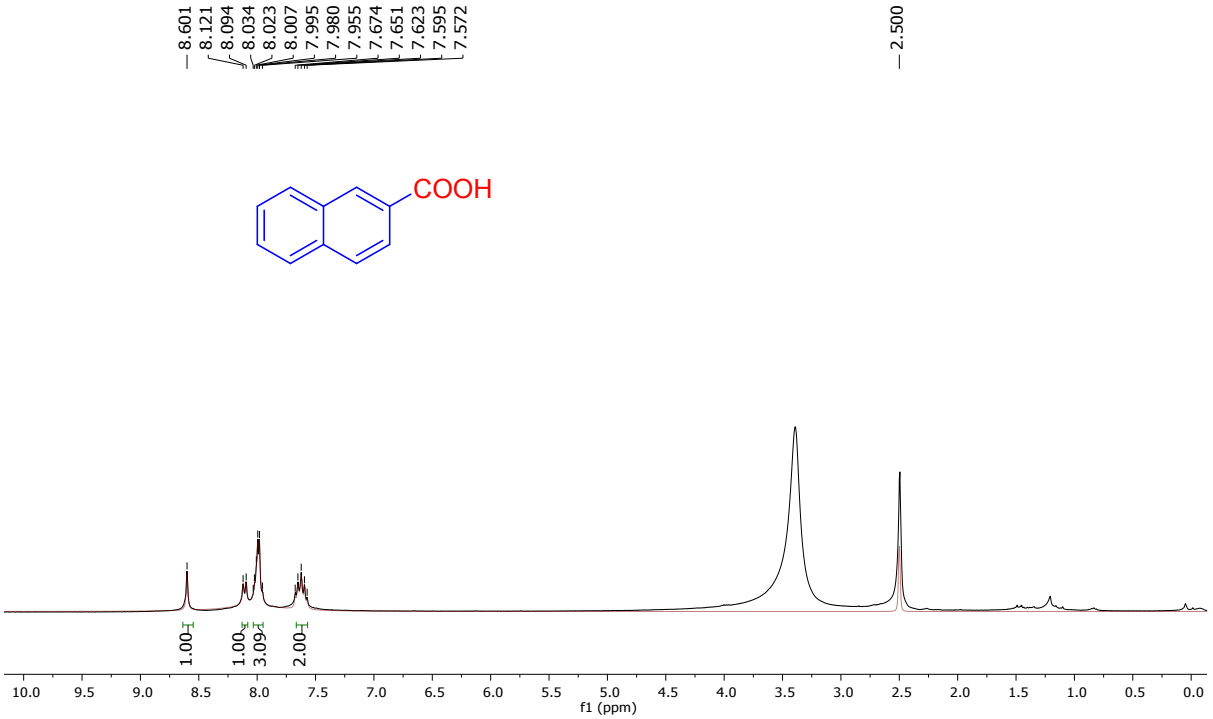


## $^{13}$C NMR

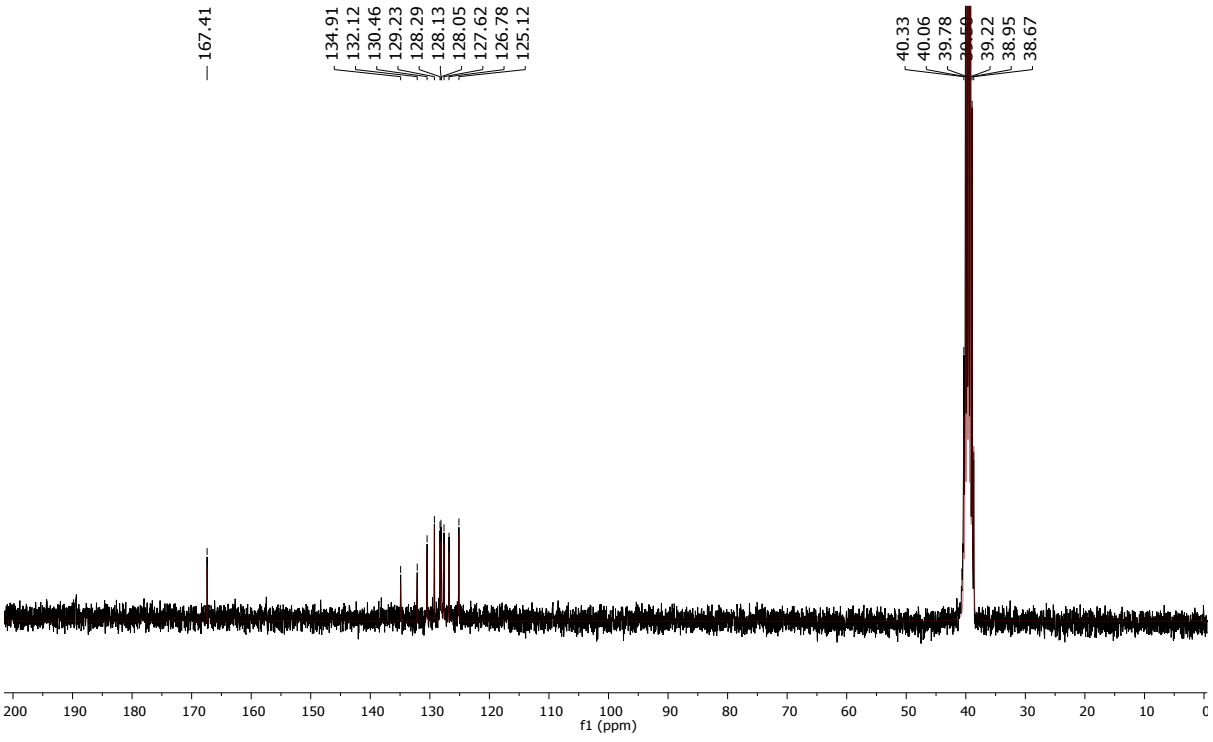


## Acetophenone (2l)

## $^{1}$H NMR

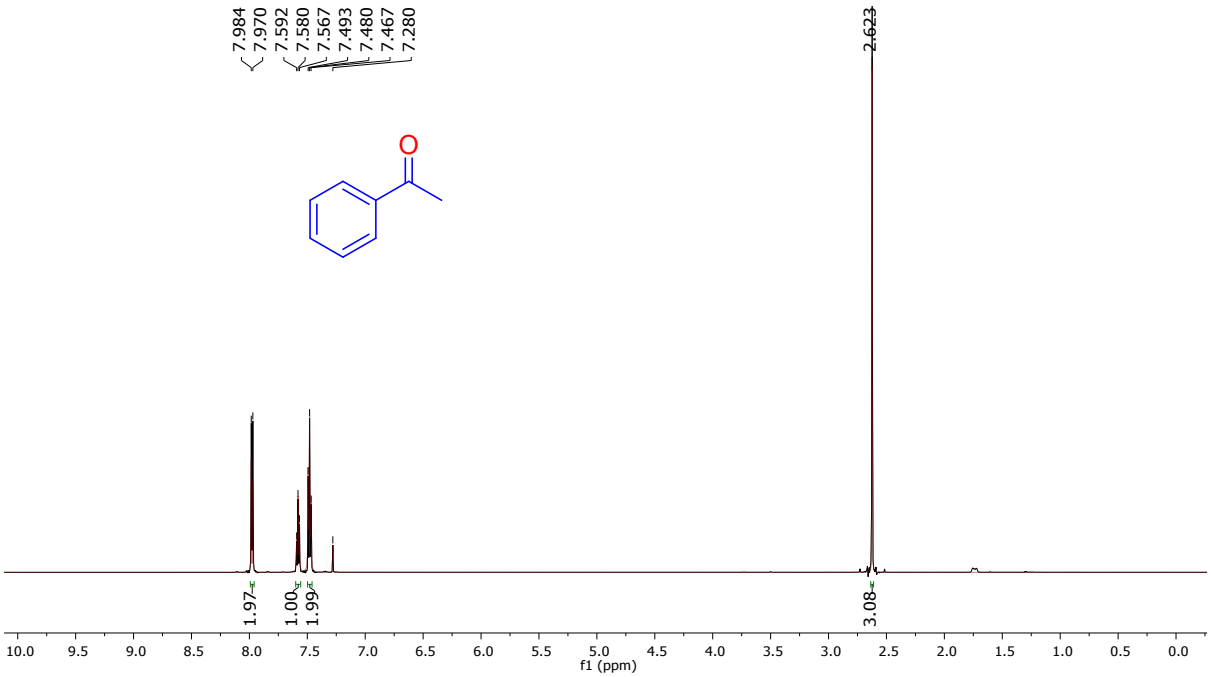


## $^{13}$C NMR

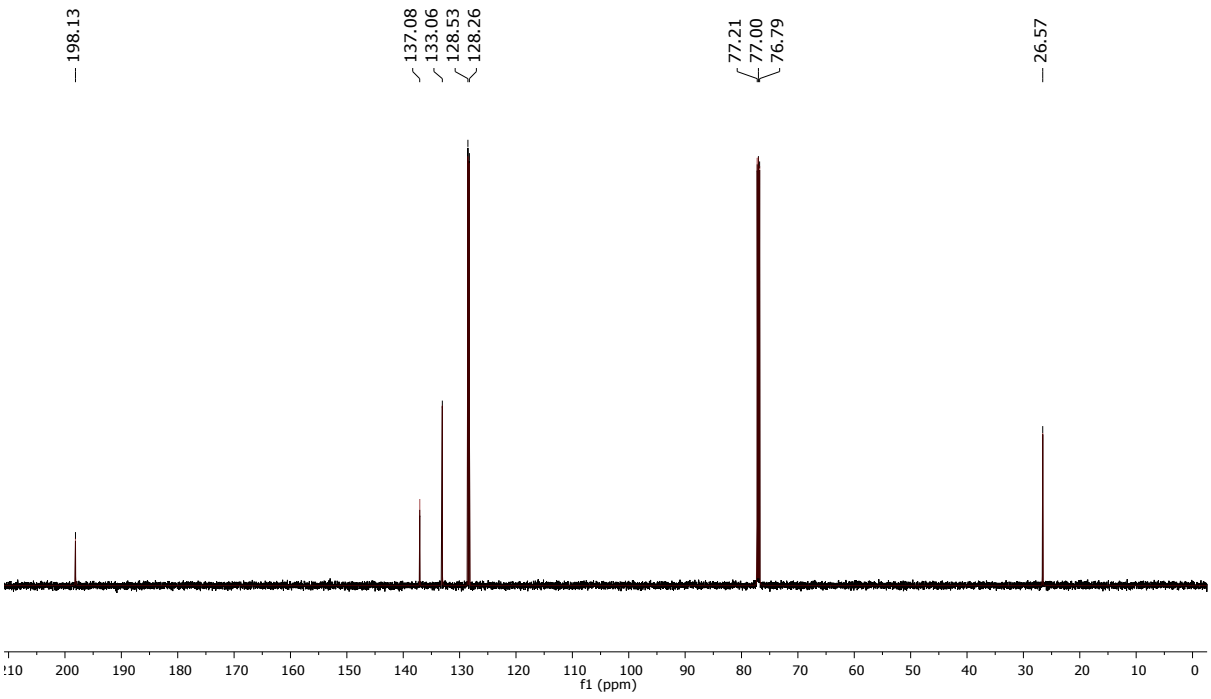


## 4-((2-methoxy-2-oxoethyl)carbamoyl)benzoic acid (2m)

## $^{1}$H NMR

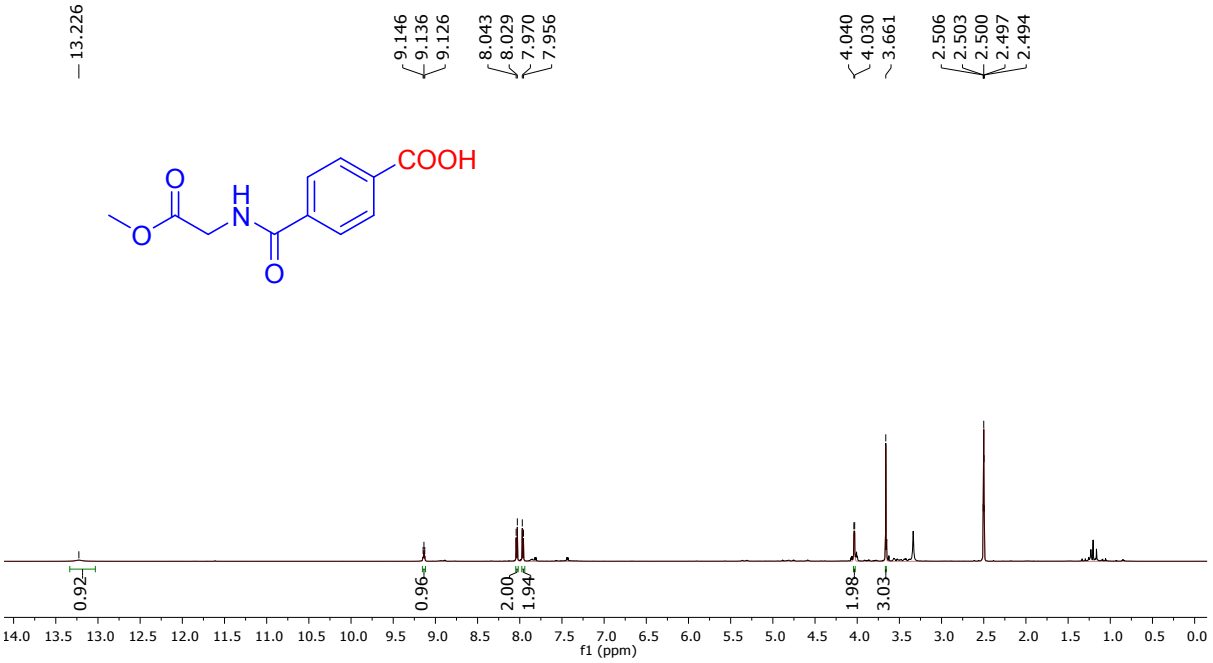


## $^{13}$C NMR

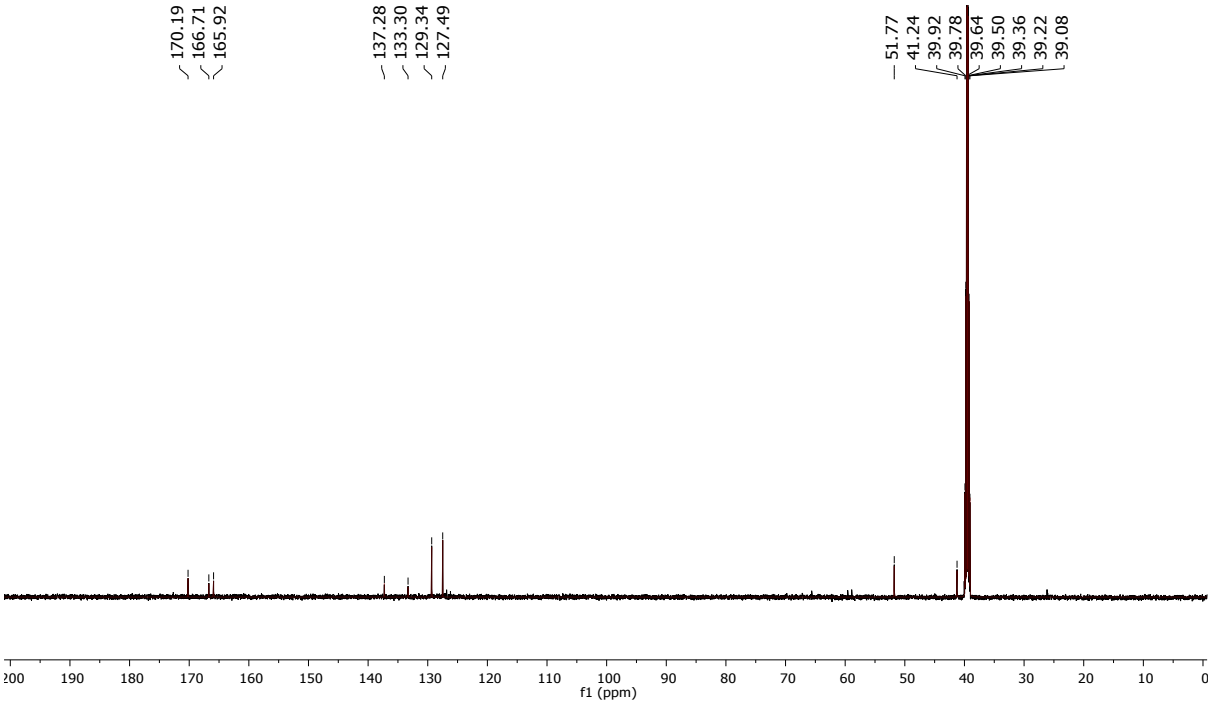


**(*S*)-4-((1-methoxy-1-oxopropan-2-yl)carbamoyl)benzoic acid (2n)**

## $^{1}$H NMR

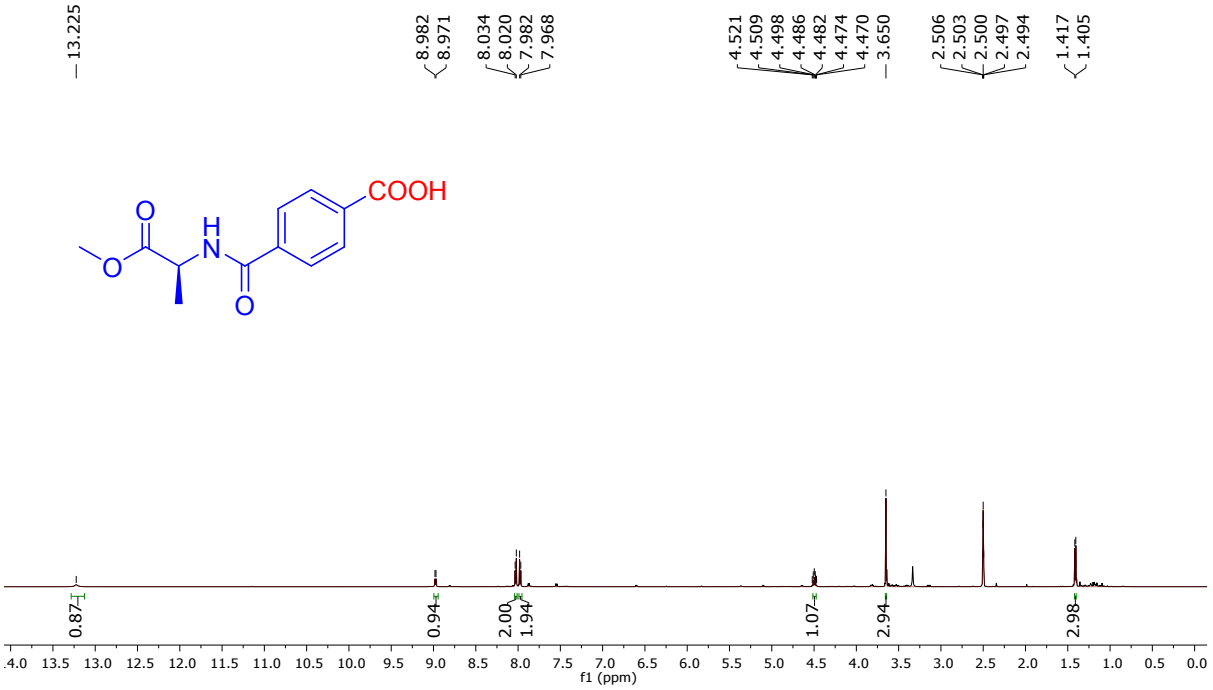


## $^{13}$C NMR

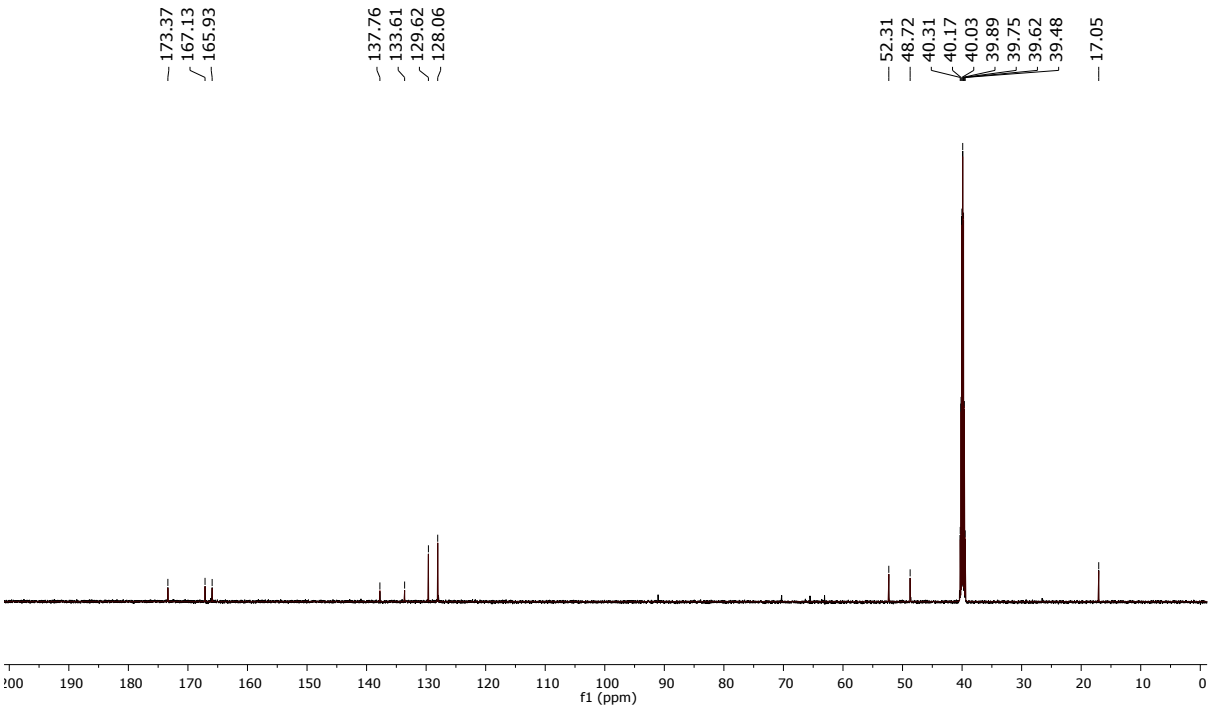


## Azelaic acid (4a)

## $^{1}$H NMR

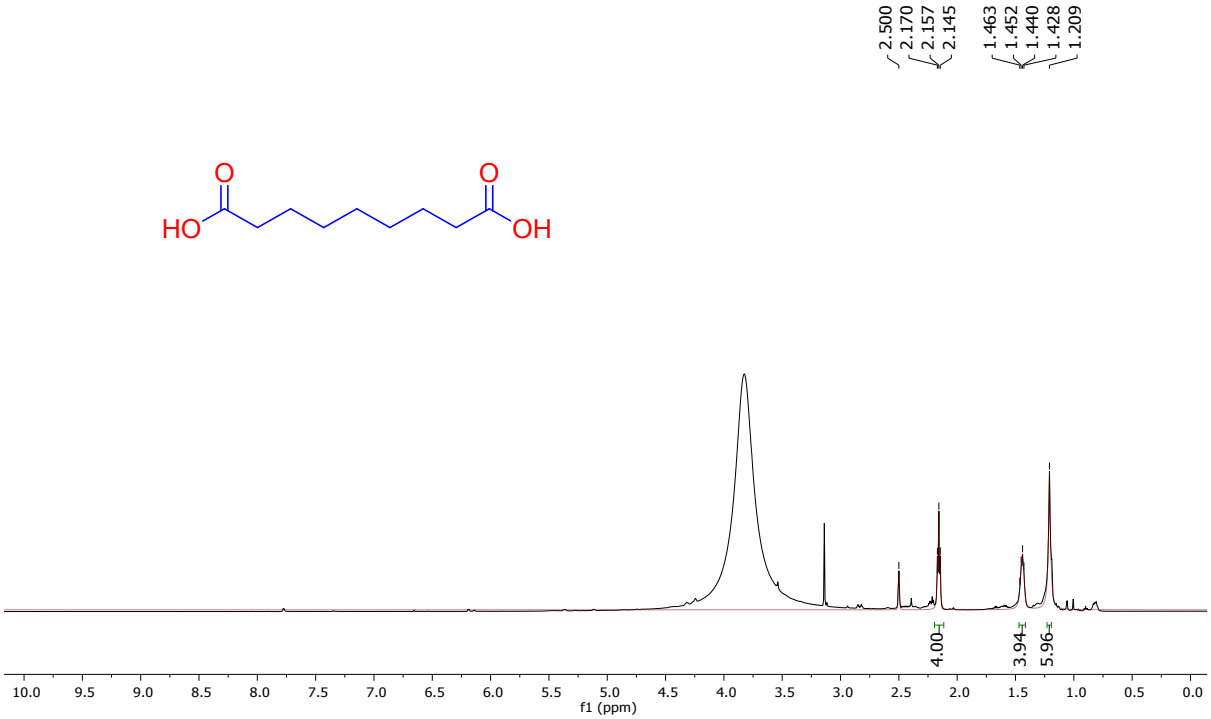


## $^{13}$C NMR

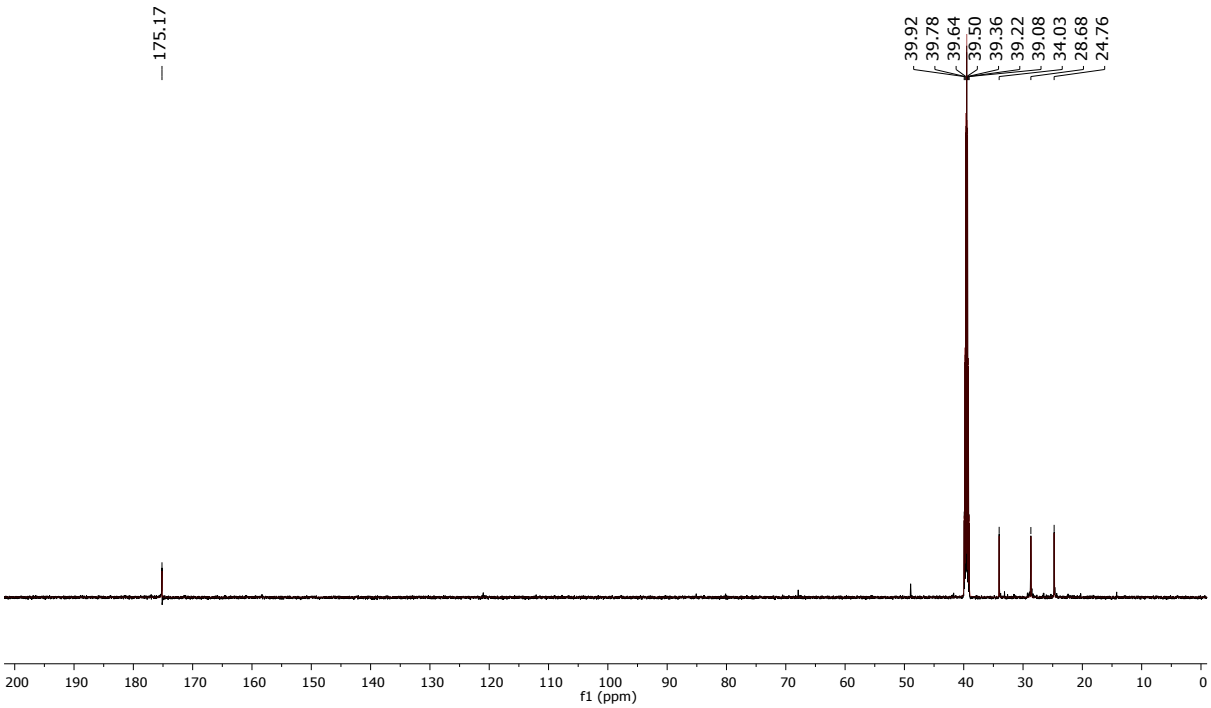


## Mass spectra of controlled experiment A

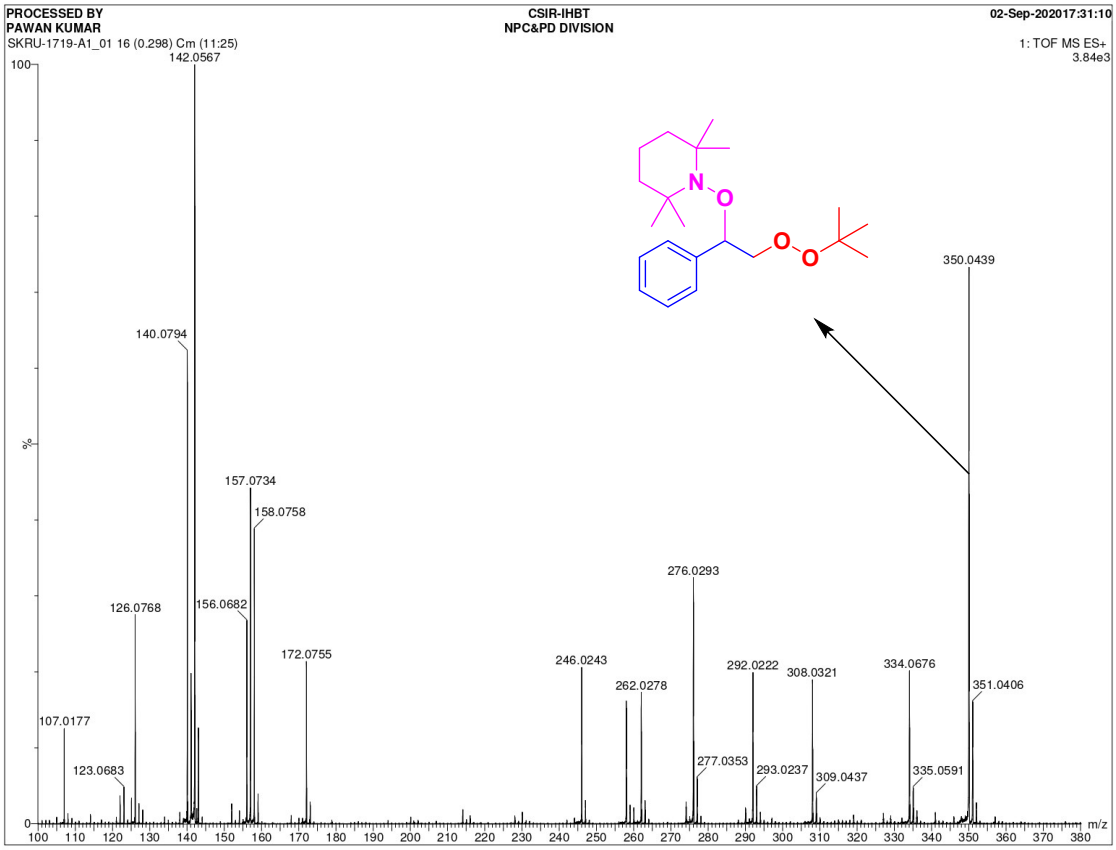


**Figure S6:** Mass spectra of controlled experiment A

## GC-MS spectra of crude reaction mixture

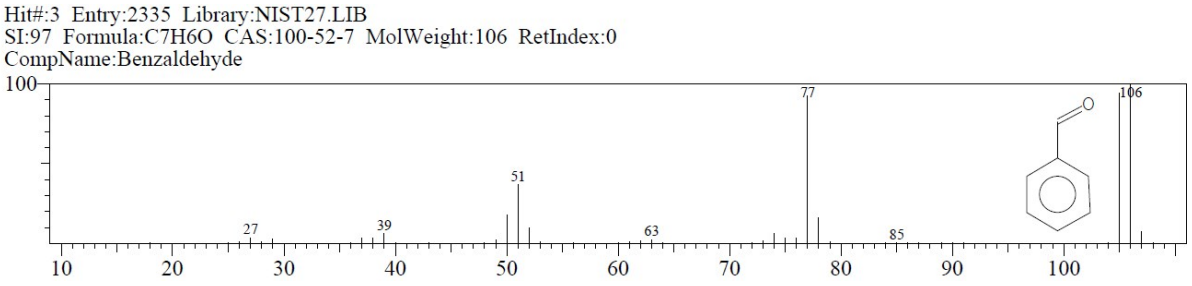


**Figure S7:** GC-MS spectra of crude reaction mixture

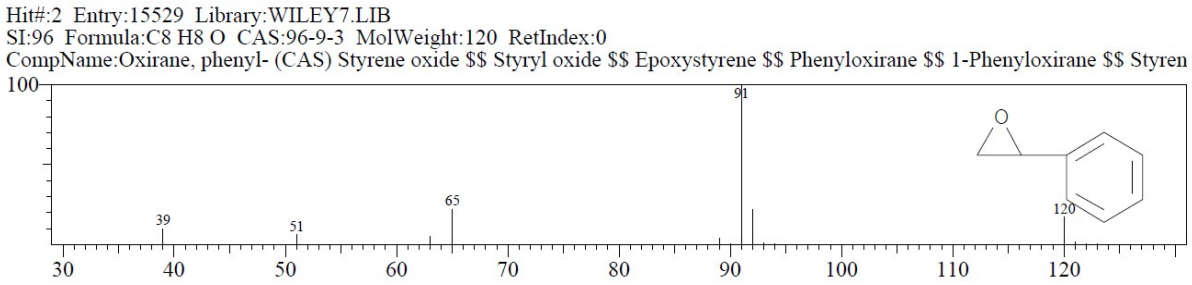


**Figure S8:** GC-MS spectra of crude reaction mixture

## References

1. E. P. Barrett, L. G. Joyner and P. P. Halenda, *J. Am. Chem. Soc.,* 1951, **73,** 373-380.

2. S. Brunaur P. H. Emmett and E. Teller, *J. Am. Chem. Soc.,* 1938, **60,** 309-319.

3. V. Singh and V. C. Srivastava, *Environ. Pollut.,* 2020, **259,** 113822.

4. S. K. Maurya, P. Patil, S. B. Umbarkar, M. K. Gurjar, M. Dongare, S. Rudiger and E. Kemnitz, *J. Mol. Catal.Chem.,* 2005, **234,** 51–57.

5. W. Zhang, G. Innocenti, P. Oulego, V. Gitis, H. Wu, B. Ensing, F. Cavani, G. Rothenberg and N. R. Shiju, *ACS Catal.* 2018, **8,** 2365-2374.

6. K. C. Soni and S. C. Shekar, *Arab. J. Chem.,* 2019, **12,** 5234-5245.

7. A. L. Patterson, *Phys Rev.,* 1939, ***56,*** 978.

8. N. D. Abazovic, M. I. Comor, M. D. Dramicanin, D. J. Jovanovic, S. P. Ahrenkiel and J. M. Nedeljkovic, *J. Phys. Chem. B,* 2006, **110,** 25366-25370.

9. S. Mugundan, B. Rajamannan, G. Viruthagiri, N. Shanmugam, R. Gobi and P. Praveen, *Appl. Nanosci.*, 2015, **5,** 449-456.

10. Y. A. Chesalov, T. V. Andrushkevich, V. I. Sobolev and G. B. Chernobay, *J. Mol. Catal.Chem.,* 2013, **380***,* 118-130.

11. P. Ruff, L. Schumacher, S. Rogg and C. Hess, *ACS Catal.* 2019, **9,** 6349-6361.

12. P. Kumar, V. C. Srivastava, I. M. Mishra, *Korean J. Chem. Eng.,* 2015, **32,** 1774-1783.

13. P. Kumar, V. C. Srivastava, I. M. Mishra, *Energy Fuels* 2015, **29,** 2664-2675.

14. H. Guo, D. Li, C. Chen, L. Jia and B. Hou, *RSC Adv.,* 2015, **5,** 64202-64207.

15. T. El-Nabarawy, A. M. Youssef and S. S. Ahmed, *Adsorp. Sci. Technol.,* 2001, **19,** 159-174.

16. J. N. Moorthy, and K. N. Parida, *J. Org. Chem.,* 2014, **79,** 11431-11439.

17. H. Miura, S. Terajima, and T. Shishido, *ACS Catal.,* 2018, **8,** 6246−6254.

18. A. Nakamura, H. Kanou, J. Tanaka, A. Imamiya, T. Maegawa and Y. Miki, *Org. Biomol. Chem.,* 2018, **16,** 541-544.

19. B. Karimi**,** F. Mansouri, and H. Vali, *ACS Appl. Nano Mater.,* 2020, **3,** 10612−10627.

20. G. Rizzo, G. Albano, M. L. Presti, A. Milella, F. G. Omenetto, and G. M. Farinola, *Eur. J. Org. Chem.,* 2020, **2020,** 6992–6996.

21. X. Li, J. C. P. Syong, and Y. Zhang, *Green Chem.,* 2018, **20,** 3619-3624.